

**HYBRID NON-DESTRUCTIVE ASSESSMENT FOR FLOW INDUCED  
VIBRATION PIPING SYSTEMS USING COUPLED  
FLUID-STRUCTURE INTERACTION**

**KONG KEEN KUAN**

**INSTITUTE OF GRADUATE STUDIES  
UNIVERSITI MALAYA  
KUALA LUMPUR**

**2020**

HYBRID NON-DESTRUCTIVE ASSESSMENT FOR FLOW INDUCED  
VIBRATION PIPING SYSTEMS USING COUPLED  
FLUID-STRUCTURE INTERACTION

KONG KEEN KUAN

THESIS SUBMITTED IN FULFILLMENT  
OF THE REQUIREMENTS  
FOR THE DEGREE OF DOCTOR OF PHILOSOPHY

INSTITUTE OF GRADUATE STUDIES  
UNIVERSITY OF MALAYA  
KUALA LUMPUR

2020  
UNIVERSITY OF MALAYA

## **ORIGINAL LITERARY WORK DECLARATION**

Name of Candidate : Kong Keen Kuan

Registration / Matric No : KHA 100068

Name of Degree : Doctor of Philosophy

Title of Project Paper / Research Report / Dissertation / Thesis (“This Work”):

Enhancement of Hybrid Non-Destructive Assessment for Flow Induced Vibration Piping Systems Using Coupled Fluid-Structure Interaction Computational Mechanics

Files of Study : Vibration

I do solemnly and sincerely declare that:

- (1) I am the sole author / writer of this Work;
- (2) This Work is original;
- (3) Any use of any work in which copyright exists was done by way of fair dealing and for permitted purposes and any excerpt or extract from, or reference to or reproduction of any copyright work has been disclosed expressly and sufficiently and the title of the Work and its authorship have been acknowledged in this Work;
- (4) I do not have any actual knowledge nor do I ought reasonably to know that the making of this work constitutes an infringement of any copyright work;
- (5) I hereby assign all and every rights in the copyright to this Work to the University of Malaya (“UM”), who henceforth shall be owner of the copyright in this Work and that any reproduction or use in any form or by any means whatsoever is prohibited without the written consent of UM having been first had and obtained;
- (6) I am fully aware that if in the course of making this Work I have infringed any copyright whether intentionally or otherwise, I may be subject to legal action or any other action as may be determined by UM.

Candidate Signature :

Date :

Subscribed and solemnly declared before,

Witness’s signature :

Date :

Name :

Designation :

## ABSTRACT

Pipelines and piping systems are of great importance in many industries such as water supply, petroleum and petrochemicals and nuclear power generation. They provide transport for high-velocity pressurized fluids operating under time-varying conditions. They are required to operate non-stop for a schedule of 24 hours a day, 7 days a week. Piping vibration failures have been one of the major causes of downtime, fires and explosions in industrial plant over the past 30 years. Failure of piping systems can have disastrous effects, leading to injuries and fatalities as well as to substantial cost to industry and the environment. Flow-induced vibration of the piping system is the most common causes of pipe cracking. The primary effect of flow-induced vibration is material fatigue from a large number of associated stress cycles. One of the normal ways of assessing the severity of piping vibration is to measure the associated dynamic stresses using strain gauges. However, it entails pre-determined measurement locations and depending on the complexity of the configuration, therefore this can be complicated, time-consuming, skill and experience-dependent. An alternative more objective non-destructive assessment stratagem is adopted using advanced experimental vibration analysis techniques, i.e., Operational Modal Analysis (OMA) and Operating Deflection Shape (ODS) analysis. An in-service piping system which is a highly pressurized gas transporting pipeline in an offshore platform is used as case study. An overall piping system including main pipeline and 3<sup>rd</sup> party components is investigated for problem severity identification purpose. This novel approach is complemented by Finite Element Analysis (FEA) where modal parameters such as natural frequency and mode shape extracted from OMA are used to correlate and verify the Finite Element (FE) model. Experimental based stress analysis is performed through FEA where ODS analysis result is used as initial displacement boundary condition to measure dynamic stresses. Complicated foundations

involving weak joints on seams, various materials, and fracturing could be readily modelled, thus the highest stress concentration location could be identified through this method with higher accuracy. When different operating condition cases needed to be analysed and estimated, another set of experimental data have to be obtained, hence, in such situation it is time-consuming and labour intensive. The hybrid non-destructive assessment is further enhanced where the experimental based stress analysis is replaced by computational based stress analysis which utilises coupled Fluid-Structure Interaction (FSI) analysis computational mechanics. Operating parameters of the pipe, such as operating pressure, differential pressure, valve opening and flow rate are used as input for the well correlated FE model. Experimental and computational based stress analysis results in terms of vibration displacement and dynamic stress are compared. The results are in good agreement (less than 3% differences). Computational based approach is found to be more time and cost-saving where it can also be used to determine the maximum allowable operating condition for a complex piping system through examining the calculated dynamic stress of the piping system. In conclusion, the proposed hybrid non-destructive assessment is continuously enhanced in terms of time, accuracy, labour and complexity to rectify vibration-induced stress problem of in-service piping system.

**Keywords:** flow-induced vibration, fluid-structure interaction, hybrid non-destructive assessment

## ABSTRAK

Saluran paip dan sistem paip adalah sangat penting dalam banyak industri seperti bekalan air, petroleum, petrokimia dan penjaan tenaga nuklear. Mereka menyediakan pengangkutan untuk halaju tinggi cecair bertekanan beroperasi di dalam keadaan berbagai dengan masa. Mereka dikehendaki untuk beroperasi tanpa henti untuk jadual 24 jam sehari, 7 hari seminggu. Kegagalan getaran paip telah menjadi salah satu punca utama downtime, kebakaran dan letupan di loji industri sejak 30 tahun yang lalu. Kegagalan sistem paip boleh menyebabkan akibat buruk, yang membawa kepada kecederaan dan kematian serta kos yang besar kepada industri dan alam sekitar. Getaran yang disebabkan oleh aliran paip adalah punca yang paling biasa keretakan paip. Kesan utama aliran getaran yang disebabkan oleh kelelahan bahan dari bilangan besar kitaran tekanan yang berkaitan. Salah satu cara biasa penilaian keterukan getaran paip adalah dengan mengukur ketegangan dinamik yang berkaitan dengan menggunakan alat pengukur tekanan. Walau bagaimanapun, ia memerlukan lokasi pengukuran yang telah ditentukan dan bergantung kepada kerumitan konfigurasi, oleh itu ini boleh menjadi rumit, memakan masa, dan bergantung pada kemahiran dan pengalaman. Satu penilaian alternatif yang lebih objektif tiada-kerosakan diadopsi dengan menggunakan teknik analisis getaran eksperimen maju, iaitu Analisis Modal Operasi (OMA) dan Pesongan Operasi Shape (ODS) analisis. Satu sistem paip yang masih dalam perkhidmatan, bertekanan tinggi, dan sebagai pengangkutan saluran paip gas di pelantar luar pesisir digunakan sebagai kajian kes. Sistem paip secara keseluruhan termasuk saluran paip utama dan komponen pihak ketiga diselidiki untuk tujuan identifikasi masalah keterukan. Pendekatan baru ini dilengkapi dengan Analisis Unsur Terhingga (FEA) di mana parameter modal seperti frekuensi semula jadi dan bentuk mod yang diekstrak daripada OMA digunakan untuk menghubungkan dan mengesahkan Unsur Terhingga (FE) model. Eksperimen analisis berdasarkan ketegangan

dilakukan melalui FEA dimana hasil analisis ODS digunakan sebagai keadaan sempadan perpindahan awal untuk pengukuran tekanan dinamik. Asas rumit yang melibatkan sendi lemah pada jahitan, pelbagai bahan, dan rekah dapat segera dimodelkan, sehingga lokasi tekanan paling tinggi dapat dikenal pasti melalui kaedah ini dengan ketepatan yang lebih tinggi. Apabila kes berbeza keadaan operasi yang perlu dianalisis dan dianggarkan, satu lagi set data uji kaji perlu diperolehi, oleh itu, dalam keadaan seperti itu, ia memakan masa dan tenaga. Penilaian hybrid tiada-kerosakan ditingkatkan lagi di mana eksperimen berdasarkan analisis tegangan digantikan oleh pengiraan berdasarkan analisis tegasan yang memanfaatkan analisis Bendalir-Struktur Interaksi (FSI) mekanik komputasi. Parameter operasi paip, seperti tekanan operasi, perbezaan tekanan, pembukaan injap dan kadar aliran digunakan sebagai input untuk model FE yang berkorelasi. Hasil analisis tekanan berdasarkan eksperimen dan pengiraan dari segi anjakan getaran dan tekanan dinamik dibandingkan. Hasilnya dalam perjanjian yang baik (kurang daripada 3% perbezaan). Pendekatan berasaskan pengiraan didapati penjimatan lebih banyak masa dan kos di mana ia boleh juga digunakan untuk menentukan keadaan operasi maksimum yang dibenarkan bagi sistem paip yang kompleks melalui pemeriksaan tekanan dinamik yang dikira dari sistem paip. Kesimpulannya, penilaian hybrid tiada-kerosakan yang dicadangkan itu terus dipertingkatkan dari segi masa, ketepatan, tenaga kerja dan kerumitan untuk membetulkan getaran yang disebabkan masalah tekanan dalam perkhidmatan sistem paip.

## ACKNOWLEDGEMENTS

First of all, the author would like to express his deepest gratitude to his supervisors: Prof. Dr. Ghaffar Abdul Rahman, Prof. Dr. Zubaidah Ismail and Assoc. Prof. Dr. Chong Wen Tong for offering him an opportunity to conduct this research project and experiment. Under their guidance and supervision, the author managed to overcome all the obstacles that he faced during this project. Special thanks go to Prof. Dr. Siamak Noroozi for his useful comments and ideas given to the author.

Furthermore, the author would also like to express his gratefulness to the lab mates of vibration laboratory, Dr. Ong Zhi Chao and Dr. Khoo Shin Yee. Their constructive advice, motivation, encouragement and suggestions have certainly helped the author in preparation of this thesis. In addition to that appreciation is expressed to Quadrant2 Sdn. Bhd. for providing industrial exploration. The author would like to thank the vibration engineers in the oil and gas industry especially Mr. Eng Hoe Cheng, Mr. Syed Mahathir and Mr. Mohd Bakar Mohd Mishami for sharing their experiences and knowledge in solving vibration problems.

Moreover, the author wishes to acknowledge the advice given by all the members from Advanced Shock and Vibration Research (ASVR) Group of University of Malaya and Advanced Structural Integrity and Vibration Research (ASIVR) Group of University of Malaysia Pahang. The author gratefully acknowledges the financial assistance provided by the Postgraduate Research Fund from University of Malaya. Apart from that, the author also thanks his family members and friends who have been very supportive all this while. Last but not least, the author would like to express his sincere appreciation to every party that had given support and shared their priceless knowledge with him.

## TABLE OF CONTENTS

ABSTRACT	i
ABSTRAK	iii
ACKNOWLEDGEMENTS	v
TABLE OF CONTENTS	vi
LIST OF FIGURES	x
LIST OF TABLES	xii
LIST OF SYMBOLS AND ABBREVIATIONS	xiii
ABBREVIATIONS	xvi
CHAPTER 1 INTRODUCTION AND OBJECTIVES	1
1.1 Background	1
1.1.1. Importance of piping	1
1.1.2. Causes of failures	2
1.1.3. Current method	4
1.2 Problem Statement	5
1.3 Research objectives	6
1.4 Research flow and scope	7
1.5 Thesis outline	10
CHAPTER 2 THEORETICAL BACKGROUND	11
2.1 Introduction	11

vi

2.2	Literature review	11
2.3	Piping Vibration	16
2.3.1	Standing Wave	17
2.3.2	Vortex Shedding	18
2.3.3	Piping Severity	19
2.3.4	Standard	20
2.4	Structural Dynamics/Vibration theory	21
2.4.1	Experimental Modal Analysis (EMA)	25
2.4.2	Operational Modal Analysis (OMA)	27
2.4.3	Operating Deflection Shape (ODS) Analysis	28
2.5	Finite Element Analysis (FEA)	29
2.5.1	Computational Fluid Dynamics (CFD)	34
2.5.2	Fluid-structure interaction (FSI)	42
2.5.3	Approaches to FSI problems	48
<b>CHAPTER 3 RESEARCH METHODOLOGY</b>		<b>51</b>
3.1	Introduction	51
3.2	Apparatus and Equipment Setup	51
3.2.1	Hardware Overview	51
3.2.2	Software Overview	57
3.2.3	Piping System	61
3.3	Experimental Procedure (OMA)	63

3.4	Computational/Correlation Procedure	66
3.4.1	Overview	66
3.4.2	Modelling	68
3.4.3	Mesh Generation	68
3.4.4	Convergence study	69
3.5	Stress Analysis (Experimental Based)	72
3.5.1	ANSYS Simulation-FEA	73
3.6	Stress Analysis (Computational Based)	73
3.6.1	ANSYS Simulation FSI	76
CHAPTER 4 RESULTS AND DISCUSSIONS		78
4.1	Introduction	78
4.2	Problem identification	78
4.3	Correlation	83
4.3.1	OMA results	83
4.4	Stress Analysis (Experimental based)	88
4.5	Stress Analysis (FSI based)	92
CHAPTER 5 CONCLUSIONS		96
5.1	Conclusion	96
5.2	Future recommendation	98
REFERENCE		99
APPENDIX A		108

Universiti Malaya

## LIST OF FIGURES

Figure 1-1 Research Flow Chart .....	9
Figure 2-1 Allowable piping vibration level versus frequency.....	20
Figure 2-2 Single Degree-of-Freedom System .....	23
Figure 2-3 3D brick element, 8 nodes (3D-solid) .....	31
Figure 2-4 Simulation approaches to fluid-structure interaction problems .....	49
Figure 3-1 Size of S100C Accelerometer .....	54
Figure 3-2 Mounting Techniques and Their Effect on the Frequency Response .....	55
Figure 3-3 Forming link in the project schematic achieves data transfer between the different physics and creates imported loads in the downstream simulation.....	58
Figure 3-4 Schematic of the Duplex Stainless Steel Pipe.....	62
Figure 3-5 Measurement locations, marked with dots, connected to each other with trace lines. Location of the reference DOF is pointed by the arrow, the direction of which indicates the direction part of the DOF.....	65
Figure 3-6 Methodology Overview.....	67
Figure 3-7 : Auto mesh generated in ANSYS Simulation .....	69
Figure 3-8 Comparison of ASME procedure and proposed procedure.....	72
Figure 3-9 : Pipe inlet and outlet fixed support and wall inside the piping system set for Fluid-Solid interface. ....	73
Figure 3-10 : Fluid-Structure Interaction Analysis Flow Chart.....	75
Figure 4-1 : Bump Tests on locations L <sub>1</sub> -L <sub>6</sub> are shown in (a) – (f) .....	79
Figure 4-2 : Before modification: (a) Kicker Line Drain Valve, and (b) Valve Vibration Level vs. Frequency .....	80

Figure 4-3 : After modification: (a) Kicker Line Drain Valve, and (b) Valve Vibration Level vs. Frequency .....	81
Figure 4-4 : ODS analysis for the pipe for different testing conditions.....	82
Figure 4-5 : Overlaid ODS spectrums for DSS pipe which plot into the Allowable Piping Vibration Level versus Frequency .....	84
Figure 4-6 : 1 <sup>st</sup> vibration mode at 3.60 Hz    Figure 4-7 : 2 <sup>nd</sup> vibration mode at 4.56 Hz.....	85
Figure 4-8 : 3D CAD Model of DSS Pipe .....	86
Figure 4-9 : Mesh Model of DSS Pipe.....	86
Figure 4-10 : 1st vibration mode at 3.84 Hz .....	87
Figure 4-11: 2nd vibration mode at 4.60 Hz.....	88
Figure 4-12 Overlaid ODS Result for DSS Pipe While Operating at (a) 275MMSCFD with partially-opened valve (b) 350MMSCFD with fully-opened valve.....	89
Figure 4-13 Dynamics Stress of piping operating at 3.60Hz and 4.56Hz respectively for various flow rates: (a) 275MMSCFD (partially-opened valve) (b) 350MMSCFD (fully- opened valve) .....	91
Figure 4-14 Dynamics Stress from FSI analysis of piping operating at 275MMSCFD (partially-opened valve) .....	93
Figure 4-15 Dynamics Stress from FSI analysis of piping operating at 350MMSCFD (fully- opened valve) .....	94
Figure A-1 Flow Control Valve A .....	108
Figure A-2 Flow Control Valve B .....	108

## LIST OF TABLES

Table 3-1 Material used in the investigation of the pipe.....	52
Table 3-2 The main components in the pipe as regards to vibration .....	63
Table 3-3 Main information about the measurement of the ODS.....	65
Table 3-4: Mesh Info.....	71
Table 4-1 Summary of Dynamic Stress Level for various flow rates: (a) 275MMSCFD (partially-opened valve) (b) 350MMSCFD (fully-opened valve).....	92
Table 4-2 Summary of Dynamic Stress Level for various flow rates from ODS based and FSI based: (a) 275MMSCFD (partially-opened valve) (b) 350MMSCFD (fully-opened valve).....	94

## LIST OF SYMBOLS AND ABBREVIATIONS

$V$	Fluid flow Velocity, m/s
$\rho$	Fluid density, kg/m <sup>3</sup>
$P$	Pressure, Pa (N/m <sup>2</sup> )
$\mathbb{T}$	Stress tensor, Pa (N/m <sup>2</sup> )
$f$	<u>body forces</u> acting on the fluid (per unit volume), N/m <sup>3</sup>
$\nabla$	Del operator
$t$	Time, s
$\sigma$	Decay rate, s
$k$	Stiffness, kgs <sup>-2</sup>
$\zeta$	Damping ratio, dimensionless damping
$\omega_0$	Undamped natural frequency, Hz
$\omega_d$	Damped natural frequency, Hz
$N_{st}$	Strouhal Number, dimensionless frequency
$V$	Velocity of the fluid, ms <sup>-1</sup>
$D$	Diameter, m
KE	Kinetic Energy, J
$M$	Unit conversion factor, 4636.8 for Imperial and 1000 for Metric units
$\Phi_I$	Inlet Diameter, in or m
$\Phi$	Diameter, in or m
$\Phi_o$	Outer Diameter, in or m
$y$	Valve Opening
$W$	Current flow
$W_{max}$	Flow that would pass at fully open

$F_{shed}$	Shedding Frequency
$[C]$	Damping Coefficients
$\{Q\}$	Applied Force
$\{a\}$	Displacement
$\{\dot{a}\}$	Velocity
$\{\ddot{a}\}$	Acceleration
$\{A\}$	Vector of peak displacement
$\omega_o$	Circulation Frequency
$\lambda$	Eigenvalue
$[K]$	Determinant
$a$	Speed of sound
$M$	Mach number
$\sigma_z$	Axial Pipe Stress
$\dot{u}_z$	Axial Pipe Velocity
$Q_y$	Lateral Shear Force
$\dot{u}_y$	Lateral Pipe Velocity
$M_x$	Bending Moment
$\dot{\theta}_x$	Angular Pipe Velocity
$A$	Cross Sectional Area
$E$	Young's modulus
$e$	Wall thickness
$I$	Sectional Moment Of Area,
$K$	Bulk Modulus
$R$	Inner Pipe Radius

$z$	Distance along Pipe
$\nu$	Poisson Ratio
$\sigma_{\phi}$	Hoop Stress
$\sigma_r$	Radial Stress
$u_r$	Radial Displacement

Universiti Malaya

## ABBREVIATIONS

ADC	Analog-To-Digital Converter
CFD	Computational Fluid Dynamics
CAD	Computer Aided Design
DAQ	Data Acquisition
DOF	Degrees Of Freedom
FFT	Fast Fourier Transform
FBG	Fiber-Optic Bragg Grating
FCV	Flow Control Valve
FE	Finite Element
FEA	Finite Element Analysis
FSI	Fluid structure Interaction
FRF	Frequency Response Function
ICP	Integrated Circuit Piezoelectric
MFx	MultiField
MDOF	Multiple Degree of Freedom
MIMO	Multiple-Input Multiple-Output
MMSCFD	Million Standard Cubic Feet per Day
NI-USB	National Instrument-Universal Serial Bus
NI-DAQmx	NI Measurement & Automation
ODS	Operating Deflection Shape
OMA	Operational Modal Analysis
PDE	Partial Differential Equations

SDOF	Single Degree Of Freedom
SDV	Shut Down Valve
SIMO	Single-Input Multiple-Output
SISO	Single-Input Single-Output
SSI	Stochastic System Identification
USA	United State of America

Universiti Malaya

## **CHAPTER 1 INTRODUCTION AND OBJECTIVES**

### **1.1 Background**

#### **1.1.1. Importance of piping**

Pipelines and pipe systems are of great importance in many industries such as water supply, petroleum and petrochemicals and nuclear power generation. They provide transport for a wide range of fluid substances, such as high-speed pressurized fluids operate under time-varying conditions due to valve and pump operations. They facilitate in the provision of safety function, such as cooling systems in nuclear power plants.

Failure of piping systems can have catastrophic effects, leading to damages and even fatalities as well as inflicting a substantial additional cost to the environment and the industry (Zubaidah Ismail, Doostdar, & Harun, 2012; Zubaidah Ismail & Karim, 2013; Zubaidah Ismail, Ramli, & Somarin, 2012). Piping vibration problems in operating plants have resulted in pricey unscheduled retrofits and outages (Olson, 2002). Over the past 30 years, the majority of downtime, fires and explosions in the industrial plant are caused by piping vibration failures. For example, an explosion that origin from one piping failure at a petrochemical plant in 1974 inflicted over \$114,000,000 in property damage (Garrison, 1988). Meanwhile, over 80 cases of leaks or cracks occurred in the piping systems of charging pumps in nuclear pressurized water reactor power plants over a 2-year period (Olson, 1985). Hence, it is critically important that evaluation of piping vibration amplitudes in a system be conducted to determine whether the levels are acceptable.

### **1.1.2. Causes of failures**

In a survey conducted by Kustu and Scholl (1980), the most frequently recurring problem was identified to be pipe cracking, where the major cause of which was determined to be piping vibration. Furthermore, mechanical vibration was the cause of 22.3% of all reportable occurrences involving pipes and fittings. Vibration loading, especially flow-induced or mechanical, is the most common source of high cycle fatigue (Agency, 2006). Geng et al. (2012) showed that flow-induced vibration exists commonly in multiphase flow pipelines, and the amplitude, frequency and some other characteristic parameters of pipe vibration are closely correlated with multiphase flow rate and flow regimes.

Often the failure of piping systems in the oil and gas industries result from incompatible structural stiffness between adjacent pipes or supports structures which is usually due to sub-optimal design. Factors include non-uniform mass distribution and incompatible stiffness, especially when fluid momentum becomes greater than the stiffness of the pipe and its supporting structure. This can result in large displacements that can also lead to fatigue induced failure. In such cases, the overall dynamic response is no longer be able to estimated and the system behaves in a totally dissimilar and unpredictable behaviour (Rahman, Chao, & Ismail, 2010).

One of the main causes of the unpredictable behaviour of pipes is the induced vibrations caused by the interaction between the structure (the pipe supports as well as walls of the pipe) and the fluid flowing through the pipe. Normally, the fluid behaves as turbulent flow

and exerts random pressures on the pipe walls (Blevins, 1990; Chen, 1987). However, a random response will be induced to the pipe structure which may result in resonant vibrations due to the fluid-structure interaction (FSI) including unsteady pressure on the pipe walls and flow turbulent fluctuations. Fluid-structure interaction, unsteady pressure and turbulent flow fluctuations can induce a random excitation of the pipe and support structure which can often lead to resonant vibrations. The root cause of such excitation is usually incompatible stiffness between the piping systems and their supporting structures. Such systems with weak structural integrity experience low frequency and large amplitude vibrations resulting in premature failure. Once a critical threshold value is exceeded by the turbulent flow, the pipe response can become unstable and undergoing large structural vibrations. It has been evidenced that the FSI phenomenon induces a significant response of the structure (Dai, Wang, Qian, & Gan, 2012) and changes the fluid force acting on the walls.

Mechanical vibrations and pressure pulsations in liquid-transporting pipe systems affect performance and safety. The symptoms include fatigue damage and vibration noise to pipe and supports. Other disruptions include leaking flanges, relief valve discharges, burst rupture disks and pipes jumping off their supports. FSI is feasible that it is responsible for a significant number of unexplained piping failures and other unacceptable behaviour. FSI has to be taken into account for the analysis.

Other causes of the unpredictable behaviour of pipes are high internal velocity of the fluid which can induce high instability on a pipe supported at one end and buckling on a pipe supported at both ends. This can cause severe vibration problems such as the flow-induced vibrations of a pipeline supported above ground level and conveying internal flow. Pipe vibrations caused by internal fluid pulsation may exhibit relatively large displacements and system may fail through fatigue of piping. The dynamic forces exerted by the fluid on the pipe walls can set the pipeline in motion and alter the fluid transient to a significant degree. The fluid motion conversely interacts with the fluid walls. This again alters the characteristics of the vibration of the pipeline system and can lead to structural failure. Therefore, accurate analysis of structural vibrations and fluid transients in piping requires the formulation of FSI mechanism by which fluid and piping are coupling.

### **1.1.3. Current method**

If the vibration levels are determined to be excessive, the piping configuration, piping material, support structure or span length may have to be altered in order to make the system acceptable (J. Wachel, 1981a; J. Wachel, Morton, & Atkins, 1990; J. C. Wachel, 1995). A systematic and structured assessment approach of the vibration of pipes was suggested in (Sukaih, 2002), the study shows that some of the main problems in the existing vibrating piping systems are due to poor or inadequate supporting systems.

Olson (Olson, 2002) stated that the primary effect of steady-state vibration is material fatigue from a large number of associated stress cycles. According to Vepsä (Vepsä, 2008),

the severity of vibration with respect to fatigue depends on numerous factors such as the magnitude of the stress variation caused, number of anticipated occurrences of these variations during the estimated lifetime of the piping system, and different grades of steel have different tolerance of cyclic loading. Because of the large number of stress cycles encountered in steady-state vibration, the allowable stress values must be determined from fatigue curves. More detailed testing involves obtaining (such as through the use of strain gauges) sufficient measurements to allow pipe stresses to be accurately determined (Olson, 2002). Strain measurements are very useful for determining the effect of vibrations. A piping acceptance criterion is given in terms of maximum vibratory stress, so strain measurements produce data directly applicable to them. Strain readings can also be used to determine the frequency and approximate magnitudes of pressure fluctuations inside the piping, and strain in system supports can be used to calculate vibrational loads on supports (Olson, 2002).

## **1.2 Problem Statement**

In order to determine if measured vibration amplitudes of piping systems were acceptable, the dynamic stresses caused by the vibrations should be compared to the applicable endurance limit for the piping material (J. C. Wachel, 1995). However, conventional direct measurement of the dynamic stresses entails pre-determined measurement locations and depending on the complexity of the configuration, can therefore be a time-consuming and complicated process. Therefore, assessment of the severity of vibration in pipelines is usually based on measurement of amplitude or velocity of vibration, complemented in

some cases with the frequency spectrum of vibration. This is because the stress in a piping span which is vibrating at resonance is directly proportional to the maximum vibration amplitude (displacement, velocity, or acceleration) in the span. For piping vibration, peak values need to be measured because fatigue allowable is in terms of peak stress (Olson, 2002). In order to determine if measured vibration amplitudes of piping systems are acceptable, as observed by Wachel (J. C. Wachel, 1995), the dynamic stresses caused by the vibrations should be compared to the applicable endurance limit for the piping material. Many studies on improving the dynamic performance of pipelines system are mainly focused on the structure itself, without taking into consideration of FSI (Tang, Lu, Li, & Zhang, 2011).

### **1.3 Research objectives**

High cycle fatigue in process piping often results from excessive vibration as a result of fluid flow in the piping system. One of the normal ways of assessing the severity of this vibration is to measure the stress caused by it with strain gauges. This method tends to be subjective and dependent on the skill and experience of the operator. An alternative way is to assess the stresses along the length of the structure by using a hybrid non-destructive method that utilizing the experimental method and computational techniques.

The objectives of this study are:

1. To identify flow-induced vibration problem in the piping system using hybrid non-destructive assessment.
2. To investigate the effectiveness of hybrid non-destructive assessment of flow-induced vibration piping system using experimental based stress evaluation approach.
3. To propose an enhanced cost and time effective hybrid non-destructive assessment using coupled fluid-structure interaction computational mechanics for flow-induced vibration piping system.
4. To investigate the effectiveness of the enhanced hybrid non-destructive assessment of flow-induced vibration piping system with computational based stress evaluation approach.

#### **1.4 Research flow and scope**

Based on the objectives, the research flow chart is arranged as shown in Figure 1.1. First of all, a preliminary inspection will be conducted on the piping system to the identified problematic area. The piping system is assessed using hybrid non-destructive assessments which involve different vibration analysis techniques (Experimental Modal Analysis (EMA) and Operating Deflection Shape (ODS) analysis). A validated FE model of the piping system is obtained by the correlation between experimental and computational results. Then the project is continued with two methods, which are hybrid non-destructive assessment of flow-induced vibration piping system using experimental based stress evaluation approach and hybrid non-destructive assessment using coupled FSI

computational mechanics for flow-induced vibration piping system. The effectiveness of the two methods was investigated by comparing the results obtained.

Universiti Malaya

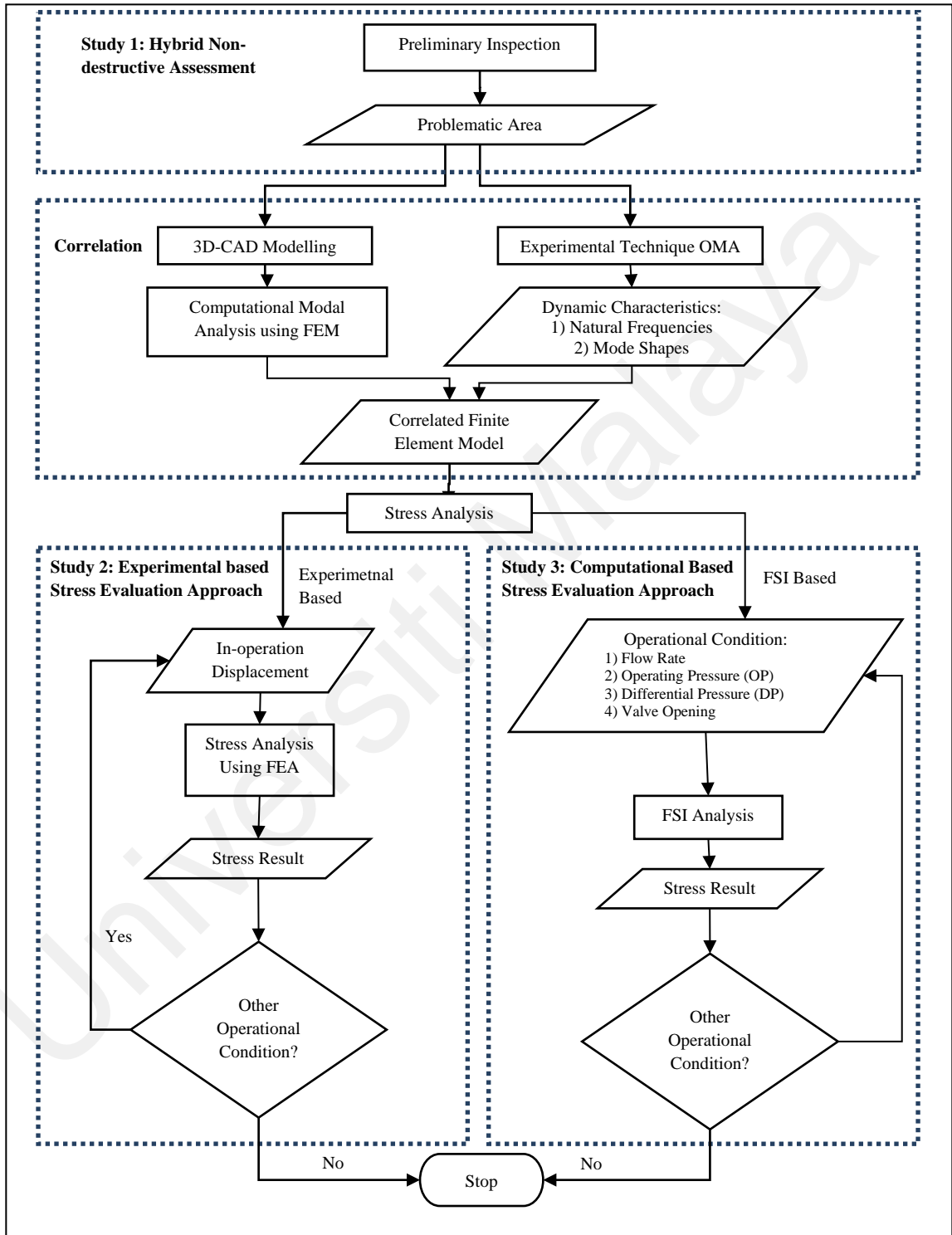


Figure 1-1 Research Flow Chart

### **1.5 Thesis outline**

The thesis is subdivided into five parts: introduction, theoretical background, research methodology, result and discussions and conclusions. The first chapter is the introduction to this research. Chapter two consists of literature reviews and the theories involved. The methodology including the materials and methods used in the research is elaborated in chapter three. Chapter four presents the results obtained with discussions. The final chapter covers the conclusions and recommendation of the work.

Universiti Malaysia

## **CHAPTER 2 THEORETICAL BACKGROUND**

### **2.1 Introduction**

In this chapter, a comprehensive literature review concerning piping vibration has been summarized and compiled. Next, the formulation and theoretical background for the piping vibration types, causes and standards used are explained in section 2.3. Structural dynamics theories are further elaborated in section 2.4. Section 2.5 covers finite element analysis (FEA) used in this research. Lastly, fluid-structure interaction related problems are discussed in section 2.6.

### **2.2 Literature review**

Conventionally, modal parameters are extracted by conducting experimental modal analysis (EMA) on a static pipe structure. Nonetheless, extracting modal parameters while the system is in operation is highly advantageous as avoiding shutting down the system. A method named operational modal analysis (OMA) has been introduced in order to analyse structures subjected to own excitation (i.e., excitation generated by their own operation) (Mohanty & Rixen, 2004). System identification methods are one of the efficient OMA tools to extract modal parameters from ambient vibrations. A full review of in-operation identification for modal analysis that is stochastic system identification (SSI) has been presented in (Peeters & De Roeck, 2001). The method described in (Trebuňa, Šimčák, Huňady, & Pástor, 2013) was successfully used to detect damages during the operation of the pipes of a gas compressor due to the flowing fluid as well as the operating equipment. When classical condition monitoring is not feasible, in-service

operating deflection shape (ODS), a non-destructive and non-invasive approach to monitor and visualise the motion of the system while in operation, (Devriendt, Steenackers, De Sitter, & Guillaume, 2010; Marscher & Jen, 1999; McHargue & Richardson, 1993; Pascual R, Golinval JC, & M, 1999) can be successfully applied.

To identify possible structural damage, fatigue growth behaviour, crack initiation and resistance of cracked pipes under cyclic loading have been studied in (Singh et al., 2003). A study that was commissioned to identify factors causing pipe failure from the aspect of microstructure and microhardness of the weld metal, weld junction, heat-affected zone and base metal was considered in (M.-B. Lin, Gao, Wang, & Volinsky, 2012). Rouabeh et al. had presented the failure analysis of a hydraulic pipe due to resonance condition as a form of energy dissipation resulting from viscous friction (Rouabeh, Schmitt, Elaoud, Hadj-Taïeb, & Pluvinaige, 2012), where a crack structural damage was identified due to the reach of maximal admissible stress and the corrosion of the pipe. Besides, a failure analysis of a natural gas pipe adjacent to a source of vibration, based on dynamic stress, modal analysis, pipe material characterisation and metallurgical assessment, was studied in (Ashrafizadeh, Karimi, & Ashrafizadeh, 2013). The main factor leading to failure (the initiation of crack) was considered as the huge energy level developed due to an escalation in the amplitude of a vibrating valve leading to the growth of the pipe dynamic stress.

Experimental and computational analysis is a common practised applied when used to study failures, such as failure analysis coal-tar coated natural gas feeder line due to vertical jetting of high-pressure erosive slurry (Mohsin, Majid, & Yusof, 2013), carbon steel pipe seriously eroded due to slurry erosion (Majid, Mohsin, & Yusof, 2012). But they are very seldom studies where both aspects of fluid and structure are considered.

Detecting, monitoring and predicting vibration (Rao & Yap, 2011) are significant and cost-effective ways to identify issues associated with structures such as incompatible structural stiffness, general wear and tear or possible imbalance problems. Nevertheless, vibration monitoring can only determine the root causes of failures which are usually triggered by poor assembly and workmanship, poor design, poor maintenance, misalignment or imbalance of whole structure of associated components. Pipes are a particular type of structure and have their own specific set of design and monitoring challenges.

The fluid-induced vibration of simply supported and clamped pipelines was studied in (Zou, Cheraghi, & Taheri, 2005), where parameters such as pipe radius to pipe-wall thickness ratio, liquid mass density to pipe-wall mass density ratio, fluid pressure and fluid velocity are considered.

Vibration analysis of a three-dimensional piping system composed of straight and curved sections is carried out in (Koo & Park, 1996) using the wave approach while the acquired results are compared with those acquired from a finite element method (FEM) formulation. Embedded Fiber-Optic Bragg Grating (FBG) sensors have been used to measure the dynamic characteristics of systems (Dong, Ibrahim, Hangzhou, & Ismail, 2013; Lou, Ibrahim, & Ismail, 2011; Luo, Ibrahim, Ismail, & Xu, 2013; Luo, Ismail, & Ibrahim, 2013; Svein, 2011). Ling et al. (Ling, Lau, Cheng, & Jin, 2006) utilized an embedded FBG sensor to measure the dynamic strain of a clamped-clamped glass fibre composite beam. A dynamic calibration test for strain measurement of the composite beam by the embedded FBG sensor and surface mounted strain gauge, at different vibration frequencies were conducted. Experimental results showed that the relationship between the photovoltage and strain measured by the embedded FBG sensor and strain gauge, respectively exhibited a linear fashion, when the strain value exceeded  $1 \mu\epsilon$ . Below this strain limit, the strain gauge could not precisely respond to the true strain of the beam. Makowski et al. (Makowski, Morawski, Michalik, & Domanski, 2011) introduced a more efficient (in terms of computing time) technique of vibration sense, based on a polar metric fibre-optic strain sensor. It was designed for localization of multiple sources of disturbances in a broad frequency spectrum without using fibre gratings. A mathematical model of the sensor is used for the development of a variational method for estimation of amplitudes of component vibrations based on noisy samples of the signal at the output of the sensor. Noda et al. (Noda et al., 2006) proposed a more accurate method of determining vibration-induced stresses by utilizing a two-mass model instead of a single-mass model

to conduct the evaluation. As mentioned earlier, all these methods require pre-determined locations where the gauges are to be attached or embedded.

Similar to other structural systems (Fayyadh, Razak, & Ismail, 2011; Z Ismail, Ibrahim, Ong, & Rahman, 2011; Zubaidah Ismail & Ong, 2012; Monajemi, Razak, & Ismail, 2013), structural health monitoring has to be continually carried out. Liu and Kleiner (Z. Liu & Kleiner, 2013) reviewed the state-of-the-art of inspection techniques and technologies towards condition assessment of water distribution and transmission mains. Several approaches of vibration-based condition monitoring and fault diagnosis of structural systems have been studied (Z. Ismail, 2012; Ong, Rahman, & Ismail, 2014; Rahman et al., 2010). Wang and Hu (Wang & Hu, 2006) studied the problem of vibration-based condition monitoring and fault diagnosis of pumps used in the oil field to recover petroleum. The vibration-based machine condition monitoring and fault diagnosis incorporate several machinery fault detection and diagnostic techniques, utilize fuzzy logic principle to increase accuracy and reduce errors caused by subjective human judgment.

The general stability problem of vibrating pipes conveying fluid has been studied comprehensively in (Blevins, 1990; Chen, 1987). The nonlinear dynamics of a curved pipe conveying fluid subject harmonic excitation was studied in (W. Lin, Qiao, & Yuying, 2007) while the nonlinear dynamics of a pulsatile pipe conveying fluid was studied in (Panda & Kar, 2008).

The phase-shift effects of resonant vibrating pipes due to various imperfections are presented in (Enz & Thomsen, 2011; Thomsen & Dahl, 2010) and their dynamic structural response in (Semke, Bibel, Jerath, Gurav, & Webster, 2006). The perturbation analysis presented provides direct insight into how the phase shift affected by the non-uniform mass, stiffness, the non-proportional damping or weak imperfections. Besides, the post-buckling effect in vibrating pipes which permit axial sliding and do not deflect transversely was discussed in (Plaut, 2006). FSI in the pipeline due to water hammer which has viscoelastic wall behaviour is studied in (Keramat, Tijsseling, Hou, & Ahmadi, 2012).

### **2.3 Piping Vibration**

Vibration exists in many piping systems in most of the industry and plants. Vibration has been identified as the dominant cause of the piping failures. Piping vibration can be caused by a weak support system that has resulted from a poor design in which vibration would occur with the normal turbulent inside the pipe. However, most cases involve good piping system design with a disturbance that is frequently generated because of a control valve in the line. The control valve could be located quite far from the observed vibration or it may be prevalent at the valve location.

The control valve can be the main causes of the flow-induced vibration of the piping system. These causes are usually the two-phase flow situations involving cavitation or flashing, standing waves within the pipe, vortex shedding and high fluid kinetic energy

(Miller, 2001). We may define the (fractional) valve opening,  $y$ , as the ratio of the current flow,  $W$ , to the flow,  $W_{max}$ , that would pass at fully open, given the same upstream conditions and throat pressure (Thomas, 1999):

$$y = \frac{W}{W_{max}} \quad (2-1)$$

### 2.3.1 Standing Wave

Within every flowing pipe, there will be a sonic wave moving axially back and forth in the pipe. This is referred to as a standing wave. The frequency of this wave will be dependent upon the length of the pipe and the sonic velocity of the fluid in the pipe. The length of the pipe is not the total length of a pipeline with all of its valves, pumps, orifices, branches and so on, but it is the length between obstructions or acoustic barriers. Examples of obstructions would be valves, pumps and orifices. An acoustic barrier would be an opening into a larger pipe, a reservoir, the end of a pipe run such as a 'T' intersection where the branch of interest requires a right-angle turn. Piping components such as expanders or reducers could be an obstruction. Any analysis should look at the frequencies with and without the expanders as obstructions. The frequency of the standing wave compared with natural frequencies of valve components and the piping system to determine if there is a potential for this to be the root cause of the vibration.

To control the vibration caused by a standing wave it is necessary to change the magnitude or the frequency of the standing wave or change the natural frequency of the pipe or components being excited by the wave. The best approach is to address the magnitude of

the standing wave. The magnitude is related to the fluid turbulent energy that is enforcing the wave. The most dominant source of this turbulence is the kinetic energy generated by the fluid jet exiting the valve trim. Thus, a valve change with a trim that reduces this jet energy will eliminate this wave influence. However, focusing on frequency is usually not beneficial. There is such a wide range of frequencies present in the turbulent flow that excitation can continue to establish a strong wave at the new frequency and causing the piping vibration.

A transient pipe wave case that occurs sometimes is referred to as a water hammer. This is an extreme example of an acoustic wave forcing piping vibration. It is caused by a sudden opening or closing of a valve (Lynch, 1991).

### **2.3.2 Vortex Shedding**

When fluid moves through a piping component that causes a change in flow direction there likely will be a separation of the fluid from the constraining wall. With the separation, a vortex is formed and then swept into the mainstream. This vortex shedding will occur at fairly well-defined dimensionless frequencies. The strength of the vortex will vary but does not need to be very strong if the shedding frequency is coincident with the natural frequency of the piping system.

The shedding frequency for a vortex,  $F_{shed}$ , is presented as

$$F_{shed} = \frac{N_{st}V}{D} \quad (2-2)$$

where  $N_{st}$  is the Strouhal number (dimensionless frequency),  $V$  is the velocity of the fluid in  $ms^{-1}$  and  $D$  is the inner diameter in  $m$ .

The frequencies resulting from vortex shedding are generally greater than the 30 Hz that would be the upper limit for most piping system natural frequencies. As noted from the Strouhal number definition, a large characteristic dimension would have to be the cause of the vortex in order to have a shedding frequency in the 8 to 12 Hz range.

Strouhal number is a dimensionless number describing oscillating flow mechanisms. The Strouhal Number,  $N_{st}$ , varies depending upon the geometry causing the separation of the boundary layer. For a circular cylinder, its value is 0.2 over a wide range of Reynolds numbers. It is usually between 0.1 and 0.3, however, there are exceptions (Blevins, 1990).

### 2.3.3 Piping Severity

The first step of the non-invasive measurement and evaluation procedure are based on the allowable levels of piping vibration versus the associated frequencies criteria shown in Figure 2-1. The criteria state that for the cases when the vibration levels were below the design line (blue line shown in Figure 2-1), very few failures may occur, and for the cases when piping vibration amplitudes at the measured frequencies are greater than the danger line (the red line Figure 2-1), piping failures are considered to be typical occurrences.

Therefore, vibration levels versus frequency criteria can be used to assess piping vibrations and to screen systems that need further analysis (J. Wachel, 1981a).

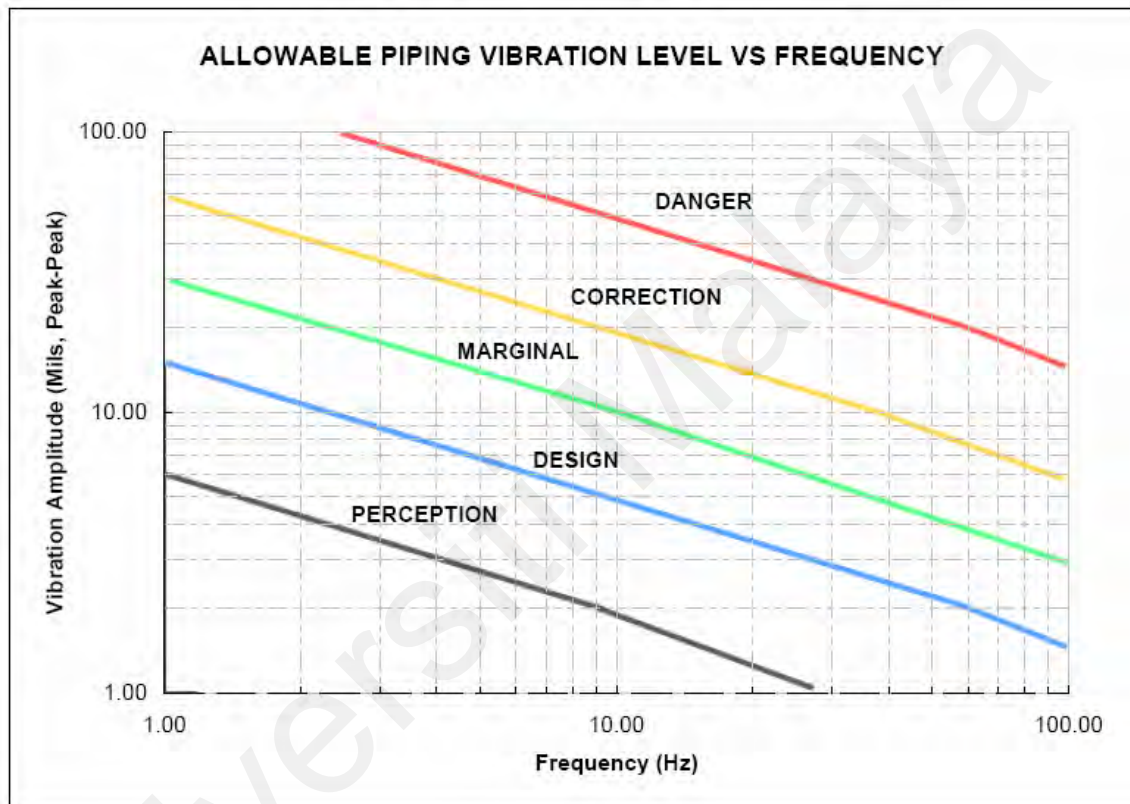


Figure 2-1 Allowable piping vibration level versus frequency

### 2.3.4 Standard

Although there are guidelines to assess the severity of vibration, these guidelines are mainly based on operational experience of the plants and they differ from source to source. What makes the estimation of the severity of vibration even more difficult is that some of the available guidelines are not stated explicitly but implicitly (Vepsä, 2008). A summary

of the guidelines or standards can be found in the work by Fomin et al. (Fomin, Kostarev, & Reinsch, 2001). According to their work, some guidelines can be used in preventing vibration-related problems to occur or when assessing the severity of vibration in existing piping systems, are presented for example in the research work by Gamble and Taggart (Gamble & Taggart Jr, 1991), the ASME B&PV section NB-3622.3 (ASME B&PV Code-III, 2007) and in the US codes ASME OM-S/G-2003 STANDARD Part 3 (OM-S/G-2003, 2004).

#### **2.4 Structural Dynamics/Vibration theory**

Structural dynamics is a subset of structural analysis which covers the behaviour of the structures subjected to dynamic loading. A modal analysis calculates the frequency modes or natural frequencies of a given system. The natural frequency of a system is dependent on the stiffness of the structure and also the mass of the structure. It is useful to know the natural frequencies of a structure to avoid resonance, which leads to large oscillations.

The response of the structure to the load is described by the theories of vibration. Vibration refers to mechanical oscillations about the equilibrium point. The oscillations may be periodic such as the motion of a pendulum.

There are two types of vibration. Free vibration occurs when a mechanical system is set off with an initial input and allowed to vibrate freely. Forced vibration is when an alternating force or motion is applied to a mechanical system. In forced vibration, the

frequency of the vibration is the frequency of the force or motion applied, with the order of magnitude being dependent on the actual mechanical system.

A mode shape is a specific pattern of vibration executed by a mechanical system at a specific frequency. Different mode shapes will be associated with different frequencies. Structural analysis consists of linear and non-linear models. Linear models use simple parameters and assume that the material is not plastically deformed. Nonlinear models consist of stressing in the material that vary with the amount of deformation. A vibrational analysis is used to test material against random vibrations, shock and impact. Each of these incidences may act on the natural frequency of the material which may cause resonance and subsequent failure.

The dynamic characteristics of a system consist of the natural frequencies, their corresponding mode shape and damping. Once these three parameters for a given system are determined, then we can define its dynamic characteristic. One degree of freedom system is first considered, as this will form the foundation for the analysis of continuous systems. An infinite degree of freedom (continuous) system can be uncoupled into  $n$  sets of Single Degree Of Freedom (SDOF) system when we deal with generalised coordinates.

The mass acts as the means for storing kinetic energy (Inertia force), the spring as the means for storing potential energy (Stiffness force) and the damper as the means to dissipate energy. A typical vibration analysis starts with the mathematical modelling of

the system and continued to the derivation of governing equations, solution of the governing equations and finally the interpretation of the results.

A general SDOF system with viscous damping is shown as below

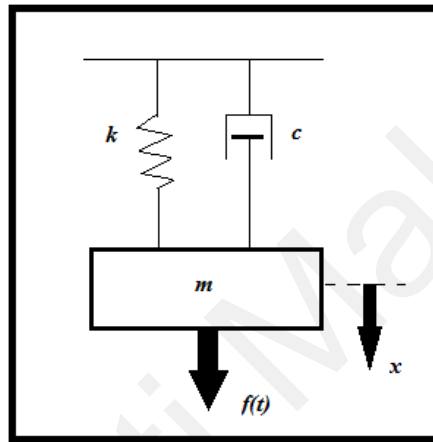


Figure 2-2 Single Degree-of-Freedom System

### Eigenvalue Analysis

The most common type of dynamic analysis for a structure is the natural frequency (eigenvalue analysis) and the corresponding mode shapes of vibration as the structure deforms in responses. For eigenvalue problems, the damping coefficients  $[C]$  and the applied force  $\{Q\}$  equal to zero. The structure starts with an initial condition of displacement  $\{a\}$ , velocity  $\{\dot{a}\}$  or acceleration  $\{\ddot{a}\}$ .

$$[M]\{\ddot{a}\} + [C]\{\dot{a}\} + [K]\{a\} = \{Q\} \quad (2-3)$$

This equation expresses the condition of free vibration, where at any instant the restoration influences in the system balance the inertia influences. The state of the natural frequency in Multiple Degree of Freedom (MDOF) system is called natural modes.

Assuming the motion of every node of the finite element model is a sinusoidal function of the peak displacement amplitude.

$$\{a\} = \{A\}\sin(\omega_0 t) \quad (2-4)$$

where  $\{A\}$  is the vector of peak displacement and  $\omega_0$  is the circulation frequency

The velocity vector,

$$\{\dot{a}\} = \{A\}\omega_0 \cos(\omega_0 t) \quad (2-5)$$

The acceleration vector,

$$\{\ddot{a}\} = -\{A\}\omega_0^2 \sin(\omega_0 t) \quad (2-6)$$

Substituting into the general equation produces the eigenvalue equation,

$$([K] - \lambda[M])\{A\} = \{0\} \quad (2-7)$$

Where the eigenvalue,  $\lambda$  is equal to  $\omega_0^2$

This equation has a trivial solution  $\{A\} = 0$ . The equation has a nontrivial solution only when determinant  $|[K] - \lambda[M]| = 0$ . The  $i$ -th nontrivial solution consists of a natural frequency of vibration and its associated mode  $\{A\}_i$ . An eigenvalue is called natural frequency  $\omega_i^2$  and its corresponding eigenvector is called mode shape.

### **2.4.1 Experimental Modal Analysis (EMA)**

Experimental Modal Analysis (EMA) is an investigation on vibration characteristics of elastic structures. EMA requires the system to be in a complete ‘shutdown’ state, which means no unaccounted excitation force induced into the system. External force such as measurable impacts or random forces are used to excite the system. The responses of the system are then cross-correlated with the measured inputs. Transfer functions are later obtained by applying the Fourier transform of the cross-correlated functions. This procedure is repeated with a different set of geometrical locations which are sufficient to represent the structure. Various curve-fitting algorithms are then used to extract the three modal parameters: namely, natural frequencies, mode shapes and modal damping.

EMA with single-input single-output (SISO), single-input multiple-output (SIMO) and multiple-input multiple-output (MIMO) modal identification algorithms in time, frequency and spatial domain have been widely used in troubleshooting, analytical model updating, structural dynamic modification, passive and active vibration control, optimal dynamic design as well as vibration-based structural health monitoring in mechanical, aerospace and civil engineering. In practical applications, the extracted modal parameters from EMA have been widely used to detect damage on beams and beam-like structures (Dilena & Morassi, 2004; Fayyadh et al., 2011; Zubaidah Ismail, 2012; Zubaidah Ismail & Ong, 2012) as well as rotor systems (Ong et al., 2014; Rahman, Ismail, Noroozi, & Chao, 2013). These are the methods used for damage detection based on dynamic characteristics of structures such as natural frequencies, dynamic mode shapes and

structural damping. The structural dynamic characteristics changes when damage event occurs, hence, this can be used as an indicator of damage.

Modal analysis is used to measure the dynamic characteristic of a system such as natural frequency, damping and mode shape. It can be divided into two types: EMA and Operational Modal Analysis (OMA). The former analysis requires a complete 'shutdown' situation of the system with no unaccounted excitation force (Ewins, 2000). EMA is conducted by using an artificial excitation with an impact hammer or shaker (Schwarz & Richardson, 1999). Instead of field testing with a large and complete system, EMA is used for lab testing of individual components or parts of the system. In this case, actual boundary conditions in lab environment may vary with the one in field environment. Therefore, boundary conditions need to be reasonably simulated when using EMA (Lingmi Zhang, Wang, & Tamura, 2010). If EMA is performed under an 'operation' situation, the induced response will be a linear superimposition of the responses due to artificial excitation, unaccounted operating forces, ambient forces, and so forth (Rahman, Ong, & Ismail, 2011). This will cause an error to the measured Frequency Response Function (FRF) which is the transfer function between output response and input force. In fact, FRF contains the information of dynamic characteristics of a system and modal parameters can be extracted from FRF by using curve-fitting algorithm. As a result, conducting EMA under an 'operation' situation always cause poor coherence result primary due to the unaccountable operating forces.

### **2.4.2 Operational Modal Analysis (OMA)**

Compared to EMA, OMA is performed under an 'operation' situation. In this case, output-only measurement (i.e. response measurement) due to the operating forces and ambient forces is needed for OMA. In this way, OMA is cheap and fast to conduct because it needs no elaborate excitation equipment and boundary condition simulation (Lingmi Zhang et al., 2010). Besides, the dynamic characteristics of a complete system can be obtained under real 'operation' situation via OMA. The operating forces acting on the in-serviced system usually cannot be measured (i.e., the sinusoidal force due to motor type excitation and broadband random excitation due to flow-induced vibration). Presently, operational modal analysis procedures are restricted to the case when excitation to the system is white stationary noise (Mohanty & Rixen, 2004). According to Zhang (Lingmi Zhang et al., 2010), system characteristics under real loading can be linearized due to broadband random excitations. The flow generated random excitation to the pipe and hence there was no issue of resonance. Resonance only occurred when cyclic excitation hitting the natural frequencies region. Therefore, ODS data was capable to reveal the mode of vibration in this case (Schwarz & Richardson, 1999). When the flow velocity is low, natural frequencies don't change much in pipeline conveying fluid (Zhai, Wu, Liu, & Yue, 2011). Random excitations are broadband excitation, able to hit all natural frequencies within the excitation range, therefore able to reveal the natural frequencies of the system in this scenario (Tongue, 2002).

### **2.4.3 Operating Deflection Shape (ODS) Analysis**

ODS can measure the deflection or animation of the structures while in-service. Generally, an ODS can be defined as ‘any forced motion of two or more points on a structure’ (Devriendt et al., 2010) and can be planar, orbital or three dimensional. ODS measurement should be carried out under constant and stable operating conditions in order to obtain accurate results as ODS represents a linear combination of the mode shapes of a structure. Therefore, the measurement should be conducted in such a way so that the measurement equipment does not have a high signal-to-noise ratio. In the measurement process, the constant and stable operating condition depends on the system complexity and whether all degrees of freedom (DOF) are measured simultaneously, while the ‘simultaneous’ condition depends on the number of data acquisition channels and DOFs to be measured.

There are basically two types of ODS, namely Time ODS which measure the vibration of a structure as a function of time, or Spectral ODS which measure the vibration pattern of an equipment (typically rotating machinery) at a specific operating frequency. For a pipe operating structure when no rotating equipment (vibration source) is used along the pipe, the measured time signal obtained from the ODS can be processed to show the pipe behaviour over time.

ODS can be defined as any forced motion of two or more DOFs (points & directions) on an in-serviced machine or structure (Vold, Schwarz, & Richardson, 2000). ODS can be divided into three categories: time-based ODS, frequency-based ODS and run-up/down

ODS. Time-based ODS is extremely useful in giving an overall ODS, which can be planar, orbital or 3D for a non-stationary signal such as a transient signal compared to frequency-based ODS. It is recommended to perform frequency-based ODS for stationary signal such as a steady-state signal under constant operating conditions.

In general, two methods of measurement are used to acquire the ODS: simultaneous method and measurement set method (Vold et al., 2000). The former method is preferred for a small-scale test object as all channels of data can be acquired at once by using a multi-channel acquisition system and hence very time efficient. However, for a large-scale test object, it is not able to acquire all data at a time. In this case, measurement set method is used. The most common measurement set method is the ODS FRF (Schwarz & Richardson, 1999). It is formed by the magnitude of auto spectrum of a roving response and the phase of the cross-spectrum between the roving response and the fixed reference response. From application point of view, the frequency-based ODS with ODS FRF is the most common method to be used for vibration monitoring of piping system in oil and gas field. Furthermore, ODS is useful in defining areas of structural weakness and also mechanical "looseness" (Sayer, 2013).

## **2.5 Finite Element Analysis (FEA)**

Finite element analysis (FEA) has become common in recent years. Numerical solutions to very complicated stress problems can now be obtained routinely using FEA.

FEA consists of a computer model of a material or design that is stressed and analysed for specific results. It is used in new structure design or existing structure refinement. Modifying an existing structure is utilized to qualify the structure for a new service condition. In the case of structural failure, FEA may be used to help to determine the design modifications to meet the new condition.

There are generally two types of analysis that are used in industry: 2-D modelling and 3-D modelling. 2-D modelling conserves simplicity and allows the analysis to be run on a relatively normal computer and it tends to yield less accurate results, while 3-D modelling produces more accurate results.

FEA uses a complex system of points called nodes which make a grid called mesh. The mesh is programmed to contain the material and structural properties which define how the structure will react to certain loading conditions. Nodes are assigned at a certain density throughout the material depending on the anticipated stress levels of a particular area. Regions which will receive a large amount of stress usually have a higher node density than those which experience little or no stress. Points of interest may consist of: fracture point of tested material, fillets, comers, complex detail and high-density areas. The mesh acts like a spider web in that from each node, there extends a mesh element to each of the adjacent nodes. This web of vectors is what carries the material properties to the object, creating many elements.

Elements fall into three major categories: 2D line elements, 2D planar elements, and 3D solid elements which are all used to define the geometry and used to apply boundary conditions. Spring elements are used to apply a specific spring constant at a specified node or set of nodes. Rigid elements are used to define a rigid connection to or in a model. The figure below shows nodes in red and the element in translucent blue.

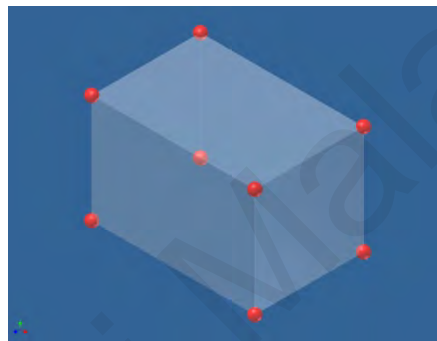


Figure 2-3 3D brick element, 8 nodes (3D-solid)

In practice, a finite element analysis usually consists of three principal steps:

1. *Pre-processing*: This is performed by constructs a model of the part to be analysed in which the geometry is divided into a number of discrete sub-regions, or “element”, connected at discrete points called “nodes.” These models can be extremely time-consuming to prepare, and commercial codes with one another to have the most user-friendly graphical “pre-processing” to assist in this rather tedious chore. Some of these pre-processors can overlay a mesh on pre-existing CAD file so that finite element analysis can be done conveniently as part of the computerized drafting-and design process.

2. *Analysis*: The dataset prepared by the pre-processor is used as input to the finite element code itself, which constructs and solves a system of linear or nonlinear algebraic equations

$$K_{ij}u_j = f_i \quad (2-8)$$

where  $u$  and  $f$  are the displacements and externally applied forces at the nodal points. The formation of the K matrix is dependent on the type of problem being attacked, and this module will outline the approach for truss and linear elastic stress analyses. Commercial codes may have very large element libraries, with elements appropriate to a wide range of problem types. Construct the global stiffness matrix. Each element matrix is assembled together to form a global matrix by equating the displacement at common nodes between adjacent elements. The size of the global matrix is equal to the total number of nodes multiplied by the number of freedom per nodes. Boundary conditions are then applied to the nodes on the structural boundary.

3. *Post processing*: A typical postprocessor display overlays coloured contours representing stress levels on the model, showing a full-filled picture similar to that of photoelastic or moiré experimental results. The solver solves a set of linear or non-linear algebraic equations simultaneously to obtain nodal results, such as displacement values at different nodes or temperature values at different nodes in a heat transfer problem. In eigenvalue problem, the eigenvalues and eigenvector are evaluated. At this point, we may interested in values of principal stresses, heat fluxes, etc.

displacement or temperature contours can be generated by interpolation of the nodal values and plotting.

### **Discretization**

The finite element method should be understood as a method for finding an approximate solution for a simplified model.

Numerical treatment reduces the simplified model to a form which is solvable by a finite number of numerical operations. This means that the approximate solution has to be characterized by a finite number of parameters  $N$ , called degrees of freedom. Such a reduction of the problem so that representation by a finite number of parameters is possible is called discretization. We expect, of course, that when  $N$  approach infinity, the finite element solutions converge to a solution which is independent of the choice of discretization. Although this phase is sometimes called finite element modelling, it is much better to call it finite element discretization, because the finite element solution approximates the exact solution of the simplified problem independently of the details of discretization, while the discretization itself does not have a meaningful physical interpretation. The numerical solution and its behaviour can and should be used for assessment for the quality of the simplified model itself. The numerical treatment should also provide some information about the accuracy and reliability of the computed data through a posteriori analysis.

### 2.5.1 Computational Fluid Dynamics (CFD)

Computational fluid dynamics (CFD) is one of the branches of fluid mechanics that uses numerical methods and algorithms to solve and analyse problems that involve fluid flows. Computers are used to perform the millions of calculations required to simulate the interaction of liquids and gases with surfaces defined by boundary conditions. Even with high-speed supercomputers, only approximate solutions can be achieved in many cases. On-going research, however, may yield software that improves the accuracy and speed of complex simulation scenarios such as transonic or turbulent flows. Initial validation of such software is often performed using a wind tunnel with the final validation coming in-flight tests.

The physical aspects of any fluid flow are governed by the following three fundamental principles: mass is conserved,  $F = ma$  (Newton's second law); and energy is conserved. These fundamental principles can be expressed in terms of mathematical equations, which in their most general form are usually partial differential equations. Computational fluid dynamics is, in part, the art of replacing the governing partial differential equations of fluid flow with numbers, and advancing these numbers in space and/or time to obtain a final numerical description of the complete flow field of interest.

Numerical methods are at the heart of the CFD process. Researchers dedicate their attention to two fundamental aspects in CFD such as physical modelling and numeric. On the other hand, the focus in numeric is to devise efficient, robust, and reliable algorithms

for the solution of partial differential equations (PDE). PDEs are a combination of differential terms (rates of change) that describe a conservation principle.

PDE in general or the governing equations in fluid dynamics, in particular, are classified into three categories: elliptic, parabolic and hyperbolic. The physical situations that these types of equations represent can be illustrated by the flow velocity relative to the speed of sound. Consider that the flow velocity  $u$  is the velocity of a body moving in the quiescent fluid. The movement of this body disturbs the fluid particles ahead of the body, setting off the propagation velocity equal to the speed of sound  $a$ . The ratio of these two competing speed is defined as Mach number,  $M$

$$M = \frac{u}{a} \quad (2-9)$$

The governing equations for subsonic flow, transonic flow, and supersonic flow are classified as elliptic, parabolic, and hyperbolic, respectively. Most of the governing equations in fluid dynamics are second order partial differential equations. The partial differential equation in a two dimensional domain are as below:

$$A \frac{\partial^2 u}{\partial x^2} + B \frac{\partial^2 u}{\partial x \partial y} + C \frac{\partial^2 u}{\partial y^2} + D \frac{\partial u}{\partial x} + E \frac{\partial u}{\partial y} + Fu + G = 0 \quad (2-3)$$

Where the coefficient  $A, B, C, D, E, F$  and  $G$  are constants or may be functions of both independent and dependent variables. To assure the continuity of the first derivative of  $u$ ,  $u_x = \partial u / \partial x$  and  $u_y = \partial u / \partial y$ ,

$$du_x = \frac{\partial u_x}{\partial x} dx + \frac{\partial u_x}{\partial y} dy = \frac{\partial^2 u}{\partial x^2} dx + \frac{\partial^2 u}{\partial x \partial y} dy \quad (2-4)$$

$$du_y = \frac{\partial u_y}{\partial x} dx + \frac{\partial u_y}{\partial y} dy = \frac{\partial^2 u}{\partial x \partial y} dx + \frac{\partial^2 u}{\partial y^2} dy \quad (2-5)$$

Here  $u$  forms a solution surface above or below the  $x$ - $y$  plane and the slope  $dy/dx$  representing the solution surface,  $s$  defined as the characteristic curve.

Equation (2.11), (2.12) and (2.13) can be combined to form a matrix equation

$$\begin{bmatrix} A & B & C \\ dx & dy & 0 \\ 0 & dx & dy \end{bmatrix} \begin{bmatrix} u_{xx} \\ u_{xy} \\ u_{yy} \end{bmatrix} = \begin{bmatrix} H \\ du_x \\ du_y \end{bmatrix} \quad (2-6)$$

Where

$$H = -(D \frac{\partial u}{\partial x} + E \frac{\partial u}{\partial y} + Fu + G) \quad (2-7)$$

Since it is possible to have discontinuities in the second-order derivatives of the dependent variable along with characteristics, these derivatives are indeterminate. This

2-D small disturbance potential equation is as below:

$$(1 - M^2) \frac{\partial^2 \phi}{\partial x^2} + \frac{\partial^2 \phi}{\partial y^2} = 0 \quad (2-8)$$

$$A = 1 - M^2, B = 0, C = 1$$

$$B^2 - 4AC = -4(1 - M^2)$$

$$\text{Elliptic} \quad M < 1$$

$$\text{Parabolic} \quad M = 1$$

$$\text{Hyperbolic} \quad M > 1$$

In CFD applications, computational schemes and specification of boundary conditions depend on the types of PDEs. In many cases, the governing equations in fluids and heat transfer are of mixed types. For this reason, selections of computational schemes and methods to apply boundary conditions are important subjects in CFD.

### **Viscous flow models**

It is noted that the 1D flow model cannot predict the effects of fluid viscosity and downstream pressure recovery for submerged flows. To validate the 1D flow assumption, a viscous flow model was built using commercial code, CFX, to calculate the transient flow through the same duckbill valve used in the 1D flow model.

### **SST $k-\omega$ turbulence model**

The Reynolds Averaged Navier-Stokes (RANS) equations were solved using a CFD solver for viscous flow. To close the RANS equations, the  $k-\omega/k-\epsilon$  blended shear stress transport (SST) turbulence model (Menter, 1994) was used here.

The  $k-\epsilon$  model (Jones & Launder, 1972) is a robust, computationally inexpensive, and has been widely used in a large variety of different flow situations (Wilcox, 2008). However, it performs poorly for complex flows involving severe pressure gradients (e.g. wall-bounded flow), separation, strong streamline curvature, and lacks sensitivity to adverse pressure gradients.

The  $k-\omega$  model (Wilcox, 2008) significantly overcomes the shortcomings of the  $k-\varepsilon$  model under the flow situations of near wall and adverse pressure gradients by solving one equation for the turbulence kinetic energy  $k$  and a second equation for the specific turbulence dissipation rate  $\omega$ . However, it is also strongly sensitive to the free-stream values,  $\omega_f$ , that are specified outside the shear layer (or the inner part of the boundary layer).

The  $k-\omega / k-\varepsilon$  blended shear stress transport (SST) turbulence model transitions smoothly switch using blending functions between the  $k-\omega$  model (Wilcox, 2008) near the wall and the  $k-\varepsilon$  model (Jones & Launder, 1972) away from the wall, avoiding the free-stream sensitivity of the  $k-\omega$  model, as well as near wall poor performance of the  $k-\varepsilon$  model. Therefore, the SST  $k-\omega$  model takes the advantage of the  $k-\varepsilon$  model in the outer part of the boundary layer. It improves the prediction of flow near the wall, as well as that of adverse pressure gradient and separated flows. Such adverse pressure gradients and flow separation may occur at the duckbill valve outlet towards the downstream water body or piping system.

### Original $k$ - $\omega$ model

The transport equations for the turbulent kinetic energy  $k$  and the specific rate of dissipation  $\omega$  (which is proportional to the turbulent kinetic energy dissipation  $\varepsilon$  over the turbulent kinetic energy  $k$ ) are typically written as (Wilcox, 2008):

$$\frac{\partial(\rho k)}{\partial t} + \frac{\partial(\rho u_j k)}{\partial x_j} = \tau_{ij} \frac{\partial u_i}{\partial x_j} - \beta^* \rho \omega k + \frac{\partial}{\partial x_j} [(\mu + \sigma_{k1} \mu_t) \frac{\partial k}{\partial x_j}] \quad (2-9)$$

$$\frac{\partial(\rho \omega)}{\partial t} + \frac{\partial(\rho u_j \omega)}{\partial x_j} = \frac{\gamma_1}{v_t} \tau_{ij} \frac{\partial u_i}{\partial x_j} - \beta_1 \rho \omega^2 + \frac{\partial}{\partial x_j} [(\mu + \sigma_{\omega 1} \mu_t) \frac{\partial \omega}{\partial x_j}]$$

### Transformed $k$ - $\varepsilon$ model

In order to combine or blend the two turbulence models, the  $k$ - $\varepsilon$  model is first transformed into a  $k$ - $\omega$  formulation. The transformed form of the  $k$ - $\varepsilon$  turbulence model is given below (Mentor, 1994):

$$\frac{\partial(\rho k)}{\partial t} + \frac{\partial(\rho u_j k)}{\partial x_j} = \tau_{ij} \frac{\partial u_i}{\partial x_j} - \beta^* \rho \omega k + \frac{\partial}{\partial x_j} [(\mu + \sigma_{k2} \mu_t) \frac{\partial k}{\partial x_j}] \quad (2-17)$$

$$\frac{\partial(\rho \omega)}{\partial t} + \frac{\partial(\rho u_j \omega)}{\partial x_j} = \frac{\gamma_2}{v_t} \tau_{ij} \frac{\partial u_i}{\partial x_j} - \beta_2 \rho \omega^2 + \frac{\partial}{\partial x_j} \left[ (\mu + \sigma_{\omega 2} \mu_t) \frac{\partial \omega}{\partial x_j} \right] + 2 \frac{\rho \sigma_{\omega 2}}{\omega} \frac{\partial k}{\partial x_j} \frac{\partial \omega}{\partial x_j}$$

### Blended $k$ - $\omega$ / $k$ - $\varepsilon$ model

The original  $k$ - $\omega$  model is multiplied by a function  $F_1$  and the transformed  $k$ - $\varepsilon$  model is multiplied by a function  $(1-F_1)$  and both are added together. The function  $F_1$  will be

designed to be one in the near wall region (inner layer) and zero away from the surface (outer layer) (Menter, 1994). The blended  $k$ - $\omega$ / $k$ - $\varepsilon$  model is thus given as (Menter, 1994):

$$\frac{\partial(\rho k)}{\partial t} + \frac{\partial(\rho u_j k)}{\partial x_j} = \tau_{ij} \frac{\partial u_i}{\partial x_j} - \beta^* \rho \omega k + \frac{\partial}{\partial x_j} [(\mu + \sigma_k \mu_t) \frac{\partial k}{\partial x_j}] \quad (2-18)$$

$$\begin{aligned} & \frac{\partial(\rho \omega)}{\partial t} + \frac{\partial(\rho u_j \omega)}{\partial x_j} \\ &= \frac{\gamma}{v_t} \tau_{ij} \frac{\partial u_i}{\partial x_j} - \beta \rho \omega^2 + \frac{\partial}{\partial x_j} \left[ (\mu + \sigma_\omega \mu_t) \frac{\partial \omega}{\partial x_j} \right] + 2(1 - F_1) \frac{\rho \sigma_{\omega 2}}{\omega} \frac{\partial k}{\partial x_j} \frac{\partial \omega}{\partial x_j} \end{aligned}$$

### The Shear Stress Transport (SST)

The  $k$ - $\omega$  based SST model accounts for the transport of the turbulent shear stress and gives highly accurate predictions of the onset and the amount of flow separation under adverse pressure gradients.

The SST model combines the advantages of the Wilcox and the  $k$ - $\varepsilon$  model but still fails to properly predict the onset and amount of flow separation from smooth surfaces. The reasons for this deficiency are given in detail in Menter (1994). The main reason is that both models do not account for the transport of the turbulent shear stress. This results in an over prediction of the eddy-viscosity. The proper transport behaviour can be obtained by a limiter to the formulation of the eddy-viscosity:

$$v_t = \frac{a_1 k}{\max(a_1 \omega, SF_2)} \quad (2-19)$$

where

$$v_t = \mu_t / \rho \quad (2-20)$$

Again  $F_2$  is a blending function similar to  $F_1$ , which restricts the limiter to the wall boundary layer, as the underlying assumptions are not correct for free shear flows.  $S$  is an invariant measure of the strain rate.

### **High Resolution**

The High Resolution transient scheme uses the second-order backward Euler scheme wherever and whenever possible and reverts to the first-order backward Euler scheme when required to maintain a bounded solution.

### **Second Order Backward Euler**

The Second Order Backward Euler scheme is also an implicit time-stepping scheme, but is second-order accurate, and is the default in ANSYS CFX. It is applicable for constant and variable timestep sizes. Like second-order advection schemes, however, it is not monotonic and is therefore inappropriate for some quantities that must remain bounded, such as turbulence quantities and volume fractions. When running the Second Order Backward Euler scheme, the transient scheme for turbulence equations will remain First Order, and the transient scheme for volume fraction equations will be set to a bounded second-order scheme, similar to the High Resolution scheme for advection. This scheme

is generally recommended for most transient runs. The commercial CFD code, CFX, was used for these RANS simulations.

### **2.5.2 Fluid-structure interaction (FSI)**

This deformation of a solid structure, in turn, changes the boundary condition of the fluid problem. The software involved in the analysis of fluid-structure interaction should provide “strong” coupling between the dynamic structure and the dynamics of the fluid. The interaction forces are immediately accounted for and their resultant motions enforced in each step. “Weak” coupling approaches refer to methods where computational structure and fluid analyses are run alternatively. The “weak” coupling is done “after” the dynamic evolution, whereas the “strong” interaction method provides for coupling during the dynamic step.

Academic research on the dynamic behaviour of the pipe system is fed by realistic problems from industry. The safe transport dangerous liquids in chemical plants, the integrity of the cooling-water system in nuclear power stations, the reliability of fuel injection systems in aircraft and intolerable pipe vibrations on offshore platforms are few examples (Bai et al., 2017; Huang, Zhao, & Chen, 2017; Latimer et al., 2018; Tijsseling, 1996).

Computational fluid dynamics and finite element analysis are two major areas of numerical simulation of physical systems. With the introduction of high-performance

computing, it has become possible to tackle systems with a coupling of fluid and structure dynamics. In all these settings the dilemma in modelling the coupled dynamics is that the fluid model is normally based on Eulerian perspective in contrast to the usual Lagrangian approach for the solid model. This makes the setup of a common variational description difficult. However, such a variational formulation of FSI is needed as the basis of a consistent approach to residual-based a posteriori error estimation and mesh adaption as well as the solution to optimal control problems by the Euler-Lagrange method.

In conventional water-hammer analyses, pipe elasticity is incorporate in the propagation speed of the pressure waves (Keramat et al., 2012; You & Inaba, 2013). Pipe inertia and axial pipe motion are not taken into account. For less restrained systems, fluid-structure interaction may become important.

Most works on transient fluid-structure interaction in liquid-filled pipes have been carried out in the time domain (De, Zhen-Qiang, Ya-Bo, & Hong, 2014). When needed, the information in the frequency domain can be deduced by using discrete Fourier transforms. The analysis is undertaken directly in the frequency domain and has the advantage of enabling dispersive terms to be included in a fully coupled manner. In principle, time-domain results can be obtained by numerical inverse Laplace transforms. Axial FSI coupling exists in the equations and also in boundary conditions. The development used herein highlights common features between analysis in the frequency domain and analysis by the method of characteristic in the time domain (L. Zhang, Tijsseling, & Vardy, 1999).

Three liquid-pipe interaction mechanisms can be distinguished: friction coupling, Poisson coupling and junction coupling. Friction coupling is the mutual friction between liquid and pipe. The more important Poisson coupling relates the pressures in the liquid to the axial stresses in the pipe through the radial contraction or expansion of the pipe wall. Poisson coupling leads to precursor waves. These are stress-wave-induced disturbances in the liquid which travel faster than the classical water hammer waves. Junction coupling acts as specific points in a pipe system such as unrestrained valves, bends and tees. The vibrating elbow is one of the examples which induce pressure waves in the liquid through a combined compressing and decompressing action (Hansson & Sandberg, 2001).

FSI in liquid-filled pipe systems is caused by three interaction mechanisms: friction coupling, Poisson coupling and junction coupling. Friction coupling is the mutual friction between the liquid and the axially vibrating pipe wall. Poisson coupling relates pressures in the liquid to axial stresses in the pipes through the radial vibrations of the pipe walls. While friction and Poisson coupling act along the entire pipe, the more important junction coupling takes place at pipe boundaries that can move, either in response to changes in fluid pressure or because of external excitation.

The in-plane vibration of planar, liquid-filled pipe systems is assumed herein to be governed by an eight-equation model that allows for axial (longitudinal) and lateral (flexural) wave propagation along each pipe in the system. Torsional and out-of-plane lateral motion is disregarded. The radial (hoop) motion is assumed to follow the liquid

and axial pipe motion quasi-statically. Axial and lateral waves do not influence each other in a straight pipe, but at an elbow, axial motion induces lateral motion and vice versa. The elbow is represented by boundary conditions coupling the axial and lateral motion of the adjacent pipes, thereby including the important FSI junction coupling. Junction coupling also takes place at closed pipe ends where liquid and axial pipe motion interacts. Poisson coupling is included in the axial equations of motion. Friction coupling is disregarded herein because it is usually relatively unimportant. The initial conditions are taken as zero.

When the fluid ceases to be wholly liquid, additional equations are needed to supplement the original eight. Simple two-phase flow equations are given for regions of distributed cavitation. Column separations, which mostly occur at pipe ends and junctions, are treated as boundary conditions.

The one-dimensional mathematical model for axial and lateral pipe motion, in the absence of cavitation, comprises eight first-order partial differential equations governing the eight unknowns: fluid pressure, fluid velocity,  $V$ , axial pipe stress,  $\sigma_z$ , axial pipe velocity,  $\dot{u}_z$ , lateral shear force,  $Q_y$ , lateral pipe velocity,  $\dot{u}_y$ , bending moment,  $M_x$ , and angular pipe velocity,  $\dot{\theta}_x$ . The model is valid for the acoustic behaviour of straight, slender, thin-walled, prismatic, liquid-filled pipes of circular cross-section. The pipe-wall material is homogeneous, isotropic, linear elastic and undergoes small deformations. Neglecting gravity (horizontal system herein) and friction terms (unimportant herein), the basic equations are

Axial motion

$$\begin{aligned} \frac{\partial V}{\partial t} + \frac{1}{\rho_f} \frac{\partial P}{\partial z} = 0 \quad \text{and} \quad \frac{\partial V}{\partial z} + \left( \frac{1}{K} + \frac{2R}{Ee} \right) \frac{\partial P}{\partial t} - \frac{2\nu}{E} \frac{\partial \sigma_z}{\partial t} = 0 \\ \frac{\partial \dot{u}_z}{\partial t} - \frac{1}{\rho_t} \frac{\partial y}{\partial x} = 0 \quad \text{and} \quad \frac{\partial \dot{u}_z}{\partial z} - \frac{1}{E} \frac{\partial \sigma_z}{\partial t} + \frac{\nu R}{Ee} \frac{\partial P}{\partial t} = 0 \end{aligned} \quad (2-21)$$

Lateral motion

$$\begin{aligned} \frac{\partial \dot{u}_y}{\partial t} + \frac{1}{\rho_t A_t + \rho_f A_f} \frac{\partial Q_y}{\partial z} = 0 \quad \text{and} \quad \frac{\partial \dot{u}_y}{\partial z} + \frac{4+3\nu}{EA_t} \frac{\partial Q_y}{\partial t} = -\dot{\theta}_x \\ \frac{\partial \dot{\theta}_x}{\partial t} + \frac{1}{\rho_t I_t} \frac{\partial M_x}{\partial z} = \frac{1}{\rho_t I_t} Q_y \quad \text{and} \quad \frac{\partial \dot{\theta}_x}{\partial z} + \frac{1}{EI_t} \frac{\partial M_x}{\partial t} = 0 \end{aligned} \quad (2-22)$$

Where  $A$  is the cross-sectional area,  $E$  is Young's modulus,  $e$  is the wall thickness,  $I$  is the sectional moment of area,  $K$  is the bulk modulus,  $R$  is the inner pipe radius,  $t$  is the time,  $z$  is the distance along the pipe,  $\nu$  is the Poisson ratio and  $\rho$  is the mass density; the subscripts f and t refer to the fluid and the structure (tube), respectively. The shear coefficient is taken as  $2(1 + \nu)/(4 + 3\nu)$

The assumed radial pipe motion is quasi-static since inertia forces in the radial direction are neglected in both the liquid and the pipe wall. The hoop stress,  $\sigma_\theta$ , the radial stress,  $\sigma_r$ , and the radial displacement,  $u_r$ , of the pipe wall are then linearly related to the pressure and the axial stress by

Radial motion

$$\sigma_{\theta} = \frac{R}{e}P, \quad \sigma_r = -\frac{3}{4}P \quad \text{and} \quad u_r = \frac{R^2}{Ee}P - \frac{vR}{E}(\sigma_z + \sigma_r) \quad (2-23)$$

By inspection, the radial stress,  $\sigma_r$ , in thin-walled pipes, is much smaller than the hoop stress,  $\sigma_{\theta}$ . It is therefore neglected herein in comparison with  $\sigma_{\theta}$  and also with  $\sigma_r$ . (Tijsseling, 2007)

### **Vibration causes**

Cavitation is a flow condition in which the static pressure is reduced as energy is used to accelerate the fluid to a higher velocity. If the static pressure drops below the fluid vapour pressure the fluid boils, creating vapour bubbles. When the fluid decelerates to the pipeline velocities there is recovery of the static pressure and the bubbles collapse when the static pressure is greater than the vapour pressure. The collapse of the bubbles is very damaging under most conditions in industrial processes. The collapse of a bubble creates very high-localized stress that fatigue small chunks of material from the adjacent surface.

Standing wave refers to every flowing pipe there will be a sonic wave moving axially back and forth in the pipe. The frequency of this wave will be dependent upon the length of the pipe and the sonic velocity of the fluid in the pipe.

When fluid moves through a piping component that causes a change in flow direction there likely will be a separation of the fluid from the constraining wall. With the separation, a vortex is formed and then swept into the mainstream. This vortex shedding will occur at fairly well-defined dimensionless frequencies. The strength of the vortex will vary but does not be very strong if the shedding frequency is coincident with the natural frequency of the piping system (Miller, 2001).

### **2.5.3 Approaches to FSI problems**

Fluid-structure interaction (FSI), which exists in many scientific and engineering applications, refers to the interaction phenomenon of a movable or deformable structure with internal or surrounding fluid flow. A comprehensive study of FSI problems remains a challenge due to their strong nonlinearity and multidisciplinary nature (Bungartz, et al, 2006). For most FSI problems, analytical solutions to the model equations are impossible to be obtained. There are few attempts on modelling the FSI problems, but still limited to the simple structures (Ferras, Manso, Schleiss, & Covas, 2017; G. Liu & Li, 2011). Thus, to investigate the fundamental physics involved in the complex interaction between fluids and solids, experimental or numerical methods must usually be utilized. Often, the laboratory tests are limited in scope and expensive. Thus, in the last few decades, a large number of numerical methods have been developed for the simulation of FSI. The main driving force for development is the demand from a wide range of scientific and engineering disciplines, where FSI problems play a prominent role. Meanwhile, the considerable improvement of computational power has made large-scale FSI simulations

possible and has facilitated many realistic applications of these numerical techniques. Yet research in the fields of computational fluid dynamics and computational structural dynamics is still on-going. Most numerical simulation approaches or codes (commercially used and open-sourced) are developed focusing on some special applications. Mature formulations/models to solve FSI problems for a general-purpose of industrial applications are rare. Giannopapa (2004) summarized two main approaches used for the simulation of fluid-structure interaction problems, as shown in Figure 2-4:

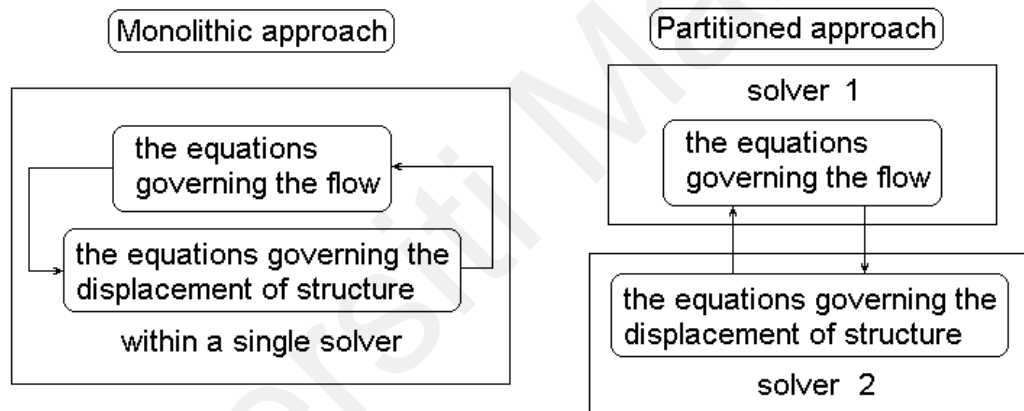


Figure 2-4 Simulation approaches to fluid-structure interaction problems

The monolithic approach solves the equations governing the fluid and the structure simultaneously within a single solver, while the partitioned approach has the equations governing the fluid and the structure solved separately with two distinct solvers. The monolithic approach requires a code developed for this particular combination of physical problems (in the fluid side or the structure side), whereas the partitioned approach utilizes

an existing fluid flow solver and structural solver and requires the development of a stable and accurate coupling algorithm.

Dynamic meshes are usually involved in FSI simulation approaches to describe the fluid and solid domains and the related fluid dynamics and structural dynamics. The emphasis of these methods is on the coordination of data transfer and consistency between the existing fluid and structural codes. Most FSI methods use the generalized Gauss-Seidel (GGS) approach for the coupled analysis, in which the fluid and structural computation are performed sequentially to achieve a multidisciplinary solution (Bungartz, et al, 2006). In other words, one may first solve the fluid field at a given time instance with an assumed interface location. The resulting fluid pressure and stress are then applied to the structure as external forces. The structural computation is then conducted to update the position of the structural surface. The new fluid mesh is then created to accommodate the new interface location. An iterative process may be required to ensure that the interfacial conditions of both the displacement and the force are satisfied at the given time instance before moving to the next time instance. The challenges that one encounters when computing employing an iterative coupled procedure are to maintain proper data transfer between the disciplines and to reach the converged solution efficiently.

## **CHAPTER 3 RESEARCH METHODOLOGY**

### **3.1 Introduction**

In this chapter, Section 3.2 will describe the apparatus and equipment used in this thesis, which includes hardware used to obtain vibration data and software to run the simulation. Then the piping system used in this study is introduced in details. Section 3.3 includes the experimental procedure to conduct OMA that was used to acquire the dynamic characteristic of the piping system. Next, Section 3.4 explains the steps for correlation of the piping systems with CAD model. Section 3.5 explains the steps for stress analysis (experimental based) and comparison to the conventional approach (ASME method), then the results are compared with stress analysis (computational based) in Section 3.6.

### **3.2 Apparatus and Equipment Setup**

#### **3.2.1 Hardware Overview**

In this thesis, the complexities of the calculations and equations can only be solved by using a computer. Finite element analysis (FEA) is a numerical technique for finding approximation solutions of partial differential equations (PDE) as well as of integral equations. Therefore, the materials used in the investigation of the pipe and the hardware requirements are tabulated as in Table 3.1.

Table 3-1 Material used in the investigation of the pipe

Instrument	Description
Wilcoxon SNAP Model S100C accelerometer	Sensitivity: 100mV/g Frequency range: 0.5-10,000Hz Amplitude range: ±80g peak
NI USB Dynamic Signal Acquisition Module, Model NI-USB 9233/9234	Number of channels: 4 ADC resolution:24 bits Type of ADC: delta sigma (with analogue pre-filtering)
DASYLab® v10.0	Sampling rate: 2000 samples per second (NI9233) Block size: 4096 samples Channel 1: impact hammer Channel 2 to channel 16: accelerometer at position 1 to 15 Averaging: 100 (for FRF measurement) Averaging: 1 (for ODS analysis) Window: Rectangular window for both excitation and response signal To perform FRF measurement and ODS analysis.

ME'scopeVES 4.0.0.99	To perform curve fitting for modal parameters extraction from FRFs data. Modal peaks function is used as mode indicator. Orthopolynomial method is used to extract damped natural frequency, damping ratio and residue mode shape.
Pro/Engineer Wildfire 5.0	To create 3D-CAD modelling
ANSYS Workbench v14.5	To perform various finite element analysis such as modal analysis, stress analysis and fluid-structure interaction analysis

### 3.2.1.1 Accelerometer

Accelerometer is one of the most commonly used sensors in vibration analysis. In this study, Wilcoxon Research SNAP Model S100C accelerometer is used as the response sensor. It is an Integrated Circuit Piezoelectric (ICP) accelerometer which has a built-in charge amplifier. Once there is a response, stressed piezoelectric quartz will emit charge proportional to acceleration. Hence, internal circuitry converts the charges into voltage (low impedance) and output through the sensor's casing. This sensor can sustain temperature within -50 °C to 80 °C. This sensor has a wide range of frequency response. It can detect signal within 0.5 to 10000.0 Hz. Besides, it has the sensitivity of 100 mV/g

and can measure acceleration up to  $784.8 \text{ ms}^{-1}$ . The size of this sensor is very small (i.e., 3.73 cm height x 1.98 cm diameter as shown in Figure 3-1). The weight of the sensor is only 45 grams and thus it is very light in weight.

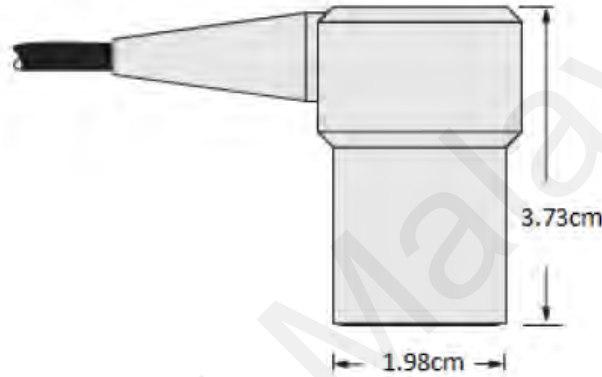


Figure 3-1 Size of S100C Accelerometer

There are several mounting methods such as probe tip, 2-pole magnet, flat magnet, mounting pad, adhesive mount, and stud mount. The mounting method of an accelerometer to a structure affects the performance of the sensor especially on the high-frequency response as shown in Figure 3-2. Considering the accessibility and flat surface of the structures, a cyanoacrylate adhesive mount with broad frequency response is chosen as the mounting method in this study so that there is no phase lag occurs during the measurement.

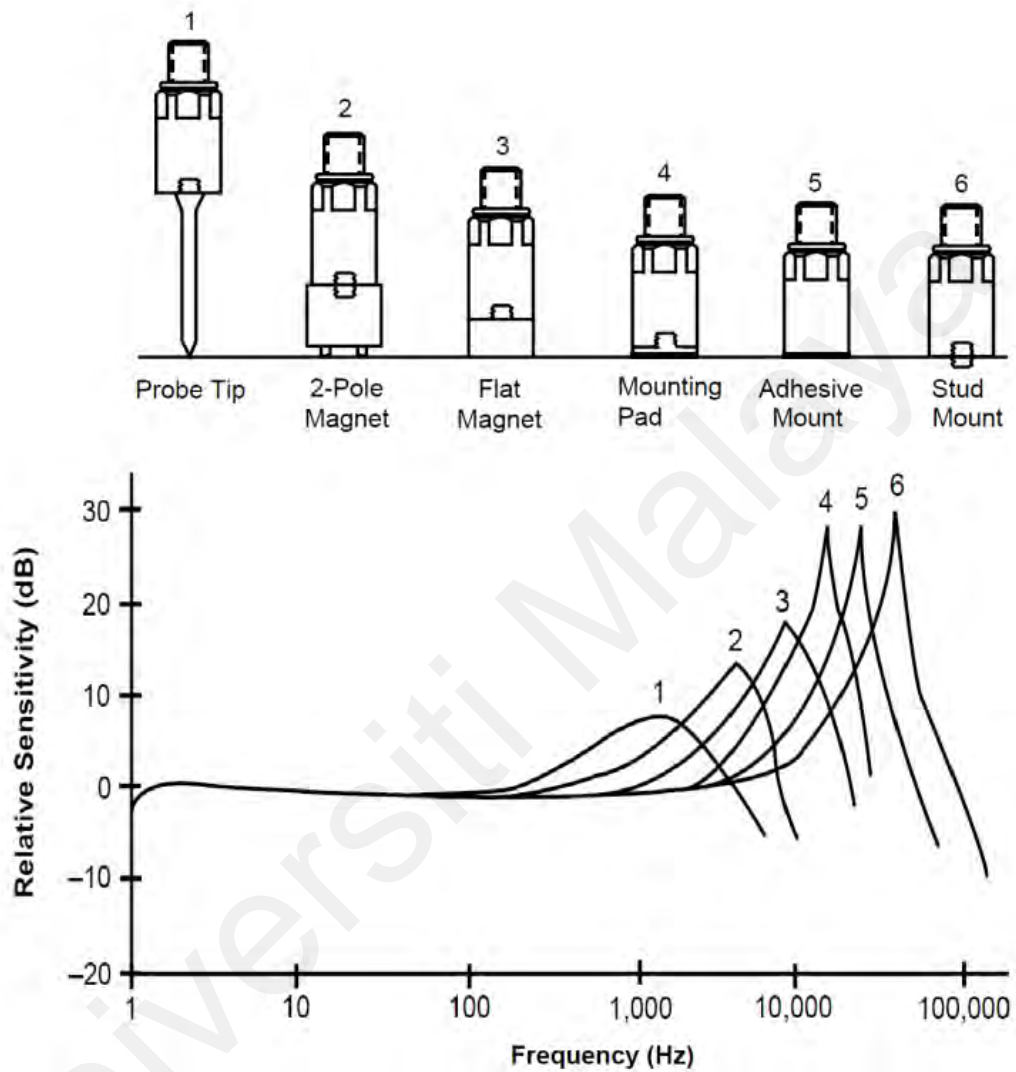


Figure 3-2 Mounting Techniques and Their Effect on the Frequency Response

### 3.2.1.2 Data Acquisition Hardware

Data acquisition (DAQ) hardware is also known as an analog-to-digital converter (ADC) which receives analog information such as response and force signals from sensors and digitize it. The digitized value will be sent to the computer and received by DAQ software. It acts as the interface between the computer and the outside world. It is a device used to digitize the incoming analog signals so that the computer can interpret them.

In this study, the National Instrument-Universal Serial Bus (NI-USB) dynamic signal acquisition module, model NI-USB 9233 is used as the DAQ hardware for acquiring the accelerometer signals. NI-USB 9233 has the capability to power up the accelerometers. It consists of 4 input channels which can simultaneously acquire signals at the rate from 2 to 50 kHz. It has a 24-bit delta-sigma ADC with analogue pre-filtered (i.e., it performs digital filtering with a cut-off frequency that automatically adjusts to the selected data rate). The sampling rate of NI-USB 9233 can be chosen within 2kS/s to 50kS/s. The NI-USB 9233 has a voltage range of  $\pm 5V$  and a dynamic range of over 100 dB. The DAQ system uses a Hi-Speed USB 2.0 connection to PC to ensure data throughput.

### **3.2.1.3 Data Acquisition Software**

Software is needed to control and drive the DAQ hardware so that the DAQ system can work properly. In this study, NI Measurement & Automation (NI-DAQmx) is used as the driver software. The function of driver software is to ease the user to communicate the DAQ hardware with the DAQ software. The driver software forms the middle layer between the application software and the hardware and enables a simple communication with no complicated programming commands to access the hardware function. Through the driver software, DAQ software such as DASyLab can be linked and conjugated to the DAQ hardware. In fact, DASyLab is a virtual instrument platform which consists of various functions such as virtual oscilloscope, virtual Fast Fourier Transform (FFT) analyser and digital filter. The flexibility in creating and modifying the instrument to fit users' needs and desires is the major advantage of a virtual instrument.

With DASyLab, user can create a software application on the computer system for FRF measurement and ODS analysis based on the theories discussed in section 2.4.3.

### **3.2.2 Software Overview**

#### **3.2.2.1 Pro/Engineer Wildfire 5.0**

Pro/ENGINEER is a parametric, integrated 3D Computer-Aided Design (CAD) solution, is used by discrete manufacturers for mechanical engineering, design and manufacturing. The parametric modelling approach uses parameters, dimensions, features, and relationships to capture intended product behaviour and create a recipe which enables design automation and the optimization of design and product development processes.

Pro/Engineer allows solid, surface and wire modelling in 3D. Solid modellers use commands to construct models that reflex manufacturing techniques, such as extrude and cut. By combining these is to make complex shapes. This is a very versatile tool in the sense that it can model virtually any geometry. Pro/ENGINEER is a fully parametric CAD program. This means that when a part is designed and modelled dimensions are assigned which define the part.

Pro/ENGINEER model can be treated as an analysis model, a part or an image. In addition, this software has a complete option to facilitate the needs of design, such as providing data (volume, density, and dimension) of the model.

### 3.2.2.2 ANSYS Workbench v14.5

The term “workbench” actually refers to a group of technologies that were created by ANSYS Inc. for developing simulation tools. An innovative project schematic view ties together the entire simulation process, guiding user every step of the way. Even complex multiphysics analyses can be performed with drag and drop simplicity. It is a new Pre/Postprocessor that is well on its way to providing a powerful and robust new front end to high-end FE analysis. Other tools such as Design Modeler, Workbench Project Page and DesignExplorer also use the same toolset.

The ANSYS Workbench platform has been engineered for scalability. Building complex, coupled analyses involving multiple physics is as easy as dragging in a follow-on analysis system and dropping it onto the source analysis. Required data transfer connections are formed automatically. As an example, consider the one-way FSI simulation shown schematically below.

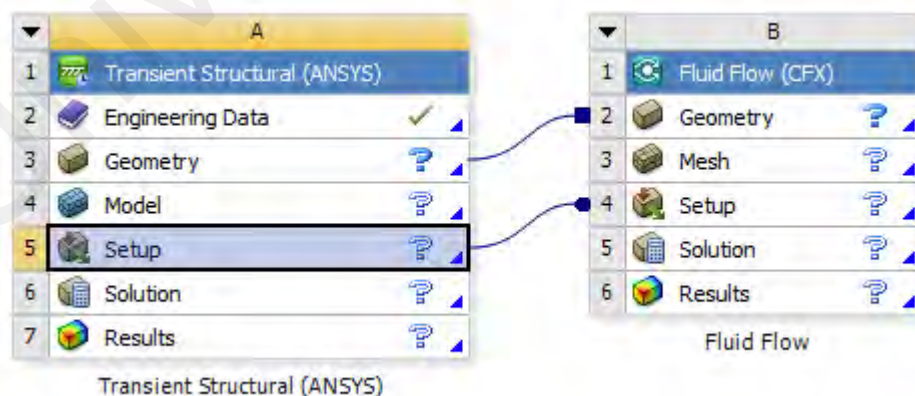


Figure 3-3 Forming link in the project schematic achieves data transfer between the different physics and creates imported loads in the downstream simulation

The ANSYS Workbench platform automatically forms a connection to share the geometry for both the fluid and the structural analyses, minimizing data storage making it easy to study the effects of geometry changes on both analyses. In addition, a connection is formed to automatically transfer pressure loads from the fluid analysis to the structural analysis.

The most significant advantages to Workbench applications are the way in which users interact with the programs while conducting a simulation. The Workbench paradigm is for users to specify objects and attributes on objects instead of the traditional command-driven approach.

### **3.2.2.3 ANSYS CFX v14.5**

ANSYS CFX is the premier Computational Fluid Dynamics (CFD) simulation program to solve the most complex fluid flow, heat transfer and chemical reaction problems. ANSYS CFX software is a high-performance, general-purpose fluid dynamics program that has been applied to solve wide-ranging fluid flow problem. At the heart of ANSYS CFX is the advanced solver technology, the key to achieving reliable and accurate solutions quickly and robustly.

ANSYS CFX is more than just a powerful CFD mode. Integration into the ANSYS Workbench platform provides superior bi-directional connections to all major CAD systems, powerful geometry modification and creation tools with ANSYS DesignModeler,

advanced meshing technologies in ANSYS Meshing, and easy drag-and-drop transfer of data and results to share between applications. For example, a fluid flow solution can be used in the definition of a boundary load of a subsequent structural mechanics simulation. A native two way connection to ANSYS structural mechanics products allows capture of even the most complex FSI problem in the same easy to use environment.

#### **3.2.2.4 ANSYS MultiField v14.5**

The ANSYS MultiField (MFX) solver enables users to solve multiphysics problems by using an automated implicit sequential coupling, which couples multiple single-physics models in one unified simulation. The ANSYS MultiField solver employs robust, iterative coupling in which each physics discipline is solved sequentially and convergence is obtained between the individual disciplines at each time point during the solution. The multifield coupling is based on customized inter-process communication technology. Coupling capabilities include thermal-structural, thermal-electric-fluid, fluid-thermal and fluid-structure interaction.

In the MFX solver is primarily intended for fluid-structure interaction analyses (including conjugate heat transfer), where the structural part using ANSYS CFX. The MFX solver can be accessed through ANSYS Simulation.

### **3.2.2.5 ANSYS Simulation**

In workbench Simulation, users read the CAD geometry, assign material properties, apply loads and boundary conditions, define mesh controls, perform solutions, review analysis results, and generate a report. This eliminates the need to switch between different software and streamlines the analysis procedures.

ANSYS Simulation offers various benefits for advanced analysis, as below:

- Faster “Initial CAD to final design” process with less effort.
- Bi-directional associativity with CAD packages
- Tight integration with other ANSYS solutions (Geometry defeaturing and modelling, Design Exploration, Fatigue Analysis, Computational Fluid Dynamics, ANSYS Meshing Technologies)
- Fully automated connection detection and creation (contact, joints)
- Increased meshing robustness and flexibility.
- Access to ANSYS functionality
- Process automation opportunity like report generation and customization wizards.

### **3.2.3 Piping System**

The piping system was a highly pressurized gas transporting pipeline in an offshore platform at Malaysia. The piping system is supported by five pipe supports and its total length is approximately 30 meters. The pipe begins from a long-distance transporting pipeline from other platform and it ends in a storage tank. The operating pressure is ranging from 4 MPa to 5 MPa and the corresponding temperature of the pipeline is

approximately 23 °C. The material of the pipe is duplex stainless steel and there is no insulation. There are two types of piping used, which are one with nominal outer diameter of the piping cross-section is 609.6 mm with the nominal value of wall thickness is 17.48 mm and the nominal outer diameter of the piping cross-section is 406.4 mm with the nominal value of wall thickness of 12.70 mm. Again, there are two nominal radii of curvature of pipe bends, which is 914.4 mm and 609.6 mm, measured from the central line of the cross-section of the pipe. The loop is shown in Figure 3-4 together with its main dimensions. Numbered arrows refer to the main components of the system. Legends for these components are listed in Table 3-2.

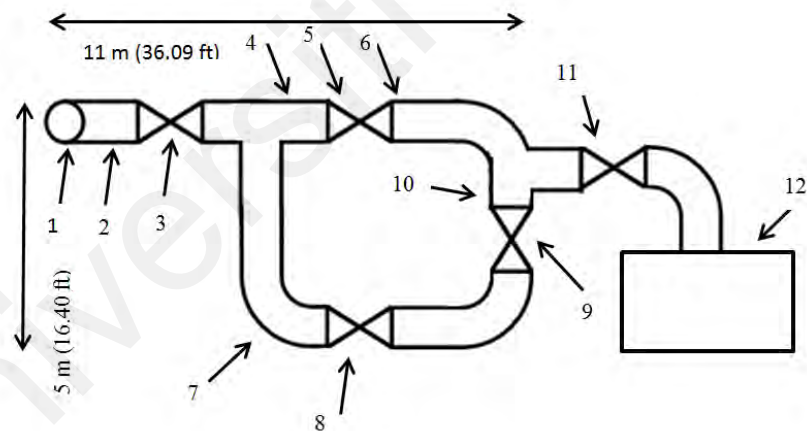


Figure 3-4 Schematic of the Duplex Stainless Steel Pipe

Table 3-2 The main components in the pipe as regards to vibration

<b>Item No.</b>	<b>Description</b>
<b>1</b>	Connection from the main feed line
<b>2</b>	1 <sup>st</sup> Pipe support
<b>3</b>	SDV (Shut Down Valve)
<b>4</b>	2 <sup>nd</sup> Pipe support
<b>5</b>	FCV (Flow Control Valve)
<b>6</b>	3 <sup>rd</sup> Pipe support
<b>7</b>	4 <sup>th</sup> Pipe support
<b>8</b>	Butterfly Valve
<b>9</b>	FCV (Flow Control Valve)
<b>10</b>	5 <sup>th</sup> Pipe support
<b>11</b>	Butterfly Valve
<b>12</b>	Storage tank

### **3.3 Experimental Procedure (OMA)**

A non-invasive evaluation and measurement procedure applied to a piping system that exhibited signs of excess fatigue was considered whether and how the stress-induced into the piping by its running conditions, i.e. flow-induced high-amplitude vibrations, affect the overall structural integrity of the piping system. The first step of the procedure covers the measurement of the subject's response to the desired loading. This step can be further divided into sub-steps of planning, data collecting, data processing and documenting. As a result of the measurements, one should obtain ODS of the subject under prevailing loading conditions. In the example discussed in this paper, the prevailing loading condition was the normal operating condition of the piping system as a whole. ODS analysis was carried out on-site on the DSS pipe to obtain the deflection pattern of the pipe while in operation. Measurements for the identification of the ODS were carried out

in 2010. Measurement points were identified and marked. All the measurement locations were taken using tri-axial accelerometer in 3 principal directions namely X, Y and Z. Main information about these measurements was collected in Table 3-3. An isometric view showing the sensor locations used in the measurements is shown in Figure 3-5. Points were linked to obtain a wire-mesh model to represent the structure as shown in Figure 3-5. All the collected data can be put into this model and visualized the vibration movement in the animation. Measurement was taken by roving accelerometer, where the reference point was fixed, and tri-axial accelerometer was switched to selected point of record. Location of the reference was pointed by arrows in Figure 3-5 with the direction of the arrow indicating the direction part of the DOF. A total of 31 points of measurement or total number of DOF of 93 was taken.

The evaluation and measurement procedure have been devised using the state-of-the-art based on a 4-channel real-time machinery analyser, modally tuned impact hammer, tri-axial (measurement locations were taken in the principal directions) and uni-axis accelerometers, and related equipment and ME'scope software (Vibrant Technology, Inc., USA) used to analyse the motion and the excessive vibration levels of the piping system. All the measurement locations were taken using tri-axial accelerometer in 3 principal directions namely X, Y and Z. Most of the measurement locations are linked to obtain a wire mesh model in software to represent the overview of the pipe as shown in Figure 3-5. After inserting the measured data into a database, this model can be used to animate and visualize the vibration movement of the piping system.

Table 3-3 Main information about the measurement of the ODS

Reference	7Y
Type of measured motion	Translational acceleration
Total number of measured DOF	93
Total number of identified ODS	9
Frequency range of the identified ODS	3.25 Hz or 22.5 Hz
Average distance between two adjacent sensors	100 cm (refer to the drawing)

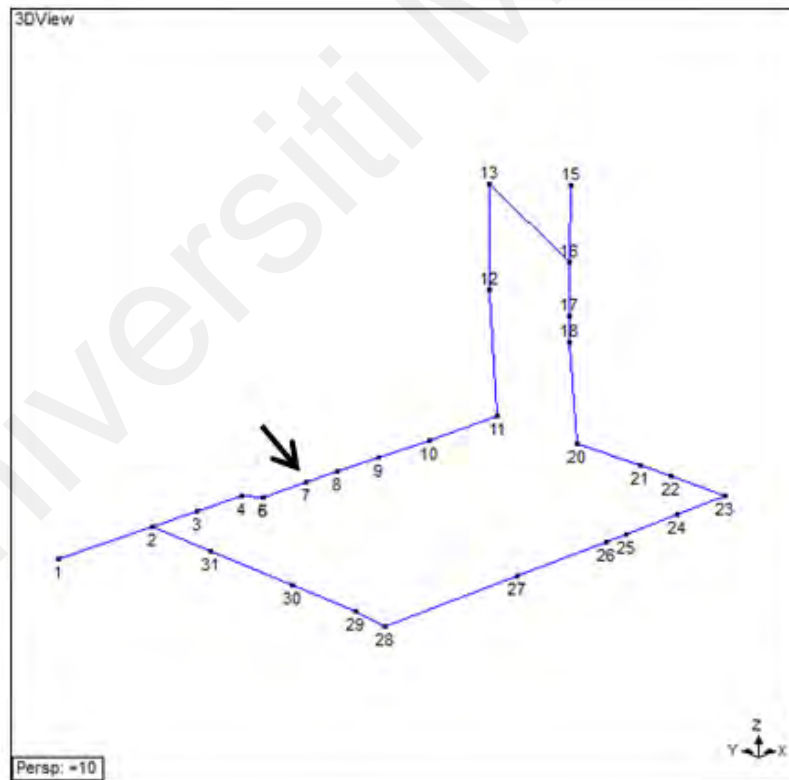


Figure 3-5 Measurement locations, marked with dots, connected to each other with trace lines. Location of the reference DOF is pointed by the arrow, the direction of which indicates the direction part of the DOF.

### **3.4 Computational/Correlation Procedure**

#### **3.4.1 Overview**

The investigation starts off by modelling the solid and fluid domain in Pro/Engineer. Then, the models are sent to the CFX-mesh for discretization. The solid region mesh is sent to ANSYS-Transient Structural analysis system for modal analysis. The structure's mode shape and corresponding natural frequency are to be found by using ANSYS- Modal analysis system. Besides that, the fluid region is sent to ANSYS-CFX to study the mass flow rate output. At last, a FSI is done on the system by using ANSYS-MultiField. The FSI setup is done at the CFX-Pre. Later, the FSI solution monitoring is done by using the CFX-Solver Manager. Finally, the post-processing result is obtained from the CFX-Post. The response of the system is analysed from the results. The methodology overview is shown in Figure 3.6.

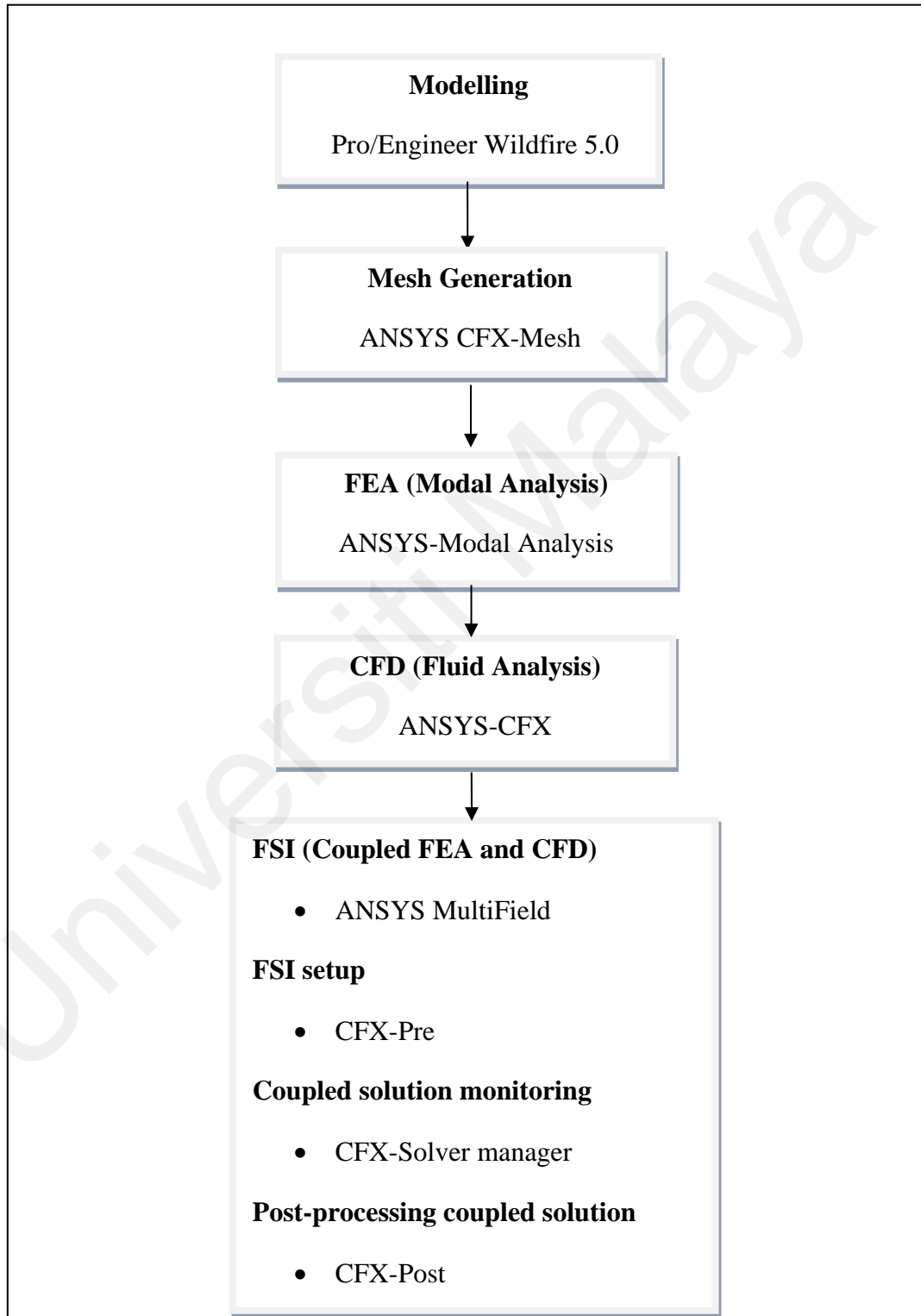


Figure 3-6 Methodology Overview

### **3.4.2 Modelling**

Modelling is to represent all the important features of a system to represent the system's behaviour at an acceptable level. The model should have enough detail to describe the system without making it too complex. The model can be improved to obtain better results.

The process started by obtaining the technical drawing of the piping system. The model is constructed by using Pro/ENGINEER. There are distinct differences when modelling for CFD and FEA analysis. The geometry for the FEA analysis is the solid model representing the structure. On the other hand, the solid model is being filled by liquid which is needed for CFD analysis. The model is exported in \*iges format and is imported into ANSYS Workbench.

### **3.4.3 Mesh Generation**

Mesh generation is an integral part of the Computational Aided Engineering (CAE) analysis process. The mesh influences the accuracy, convergence and speed of the solution. Great effort is needed for mesh generation as the time is taken to create a mesh model is a significant portion of the time it takes to obtain results from CAE solution.

The mesh quality can have an impact on the computational analysis in terms of the quality of the solution and the time needed to obtain it. The evaluation of the quality of the mesh is very useful because it provides some indication of how suitable a particular discretization is for the analysis type under consideration.

For the structural part, although there are many features to control the mesh, it does not have any problem in meshing. The built-in auto mesher in ANSYS Simulation is sufficient in producing good mesh. For the fluid part, patch conforming method and inflation are applied on the meshing in order to achieve layering and better meshing.



Figure 3-7 : Auto mesh generated in ANSYS Simulation

#### 3.4.4 Convergence study

The meshes in the simulation are generated by the ICEM CFD software packaged with the ANSYS Workbench software. For the sake of simplifying the meshing, the piping system structural domain and fluid domain are generated separately. By using the append function of the software, the meshes are merged together in the solver stage. In order to attain a reliable and promising simulation result, a finer mesh is desired; however, mesh refinement results in large data storage and a long computational time is required. Therefore, it is necessary to perform a mesh dependency test to figure out the appropriate

mesh size that provides a quality analysis while minimizing computational cost at the same time.

In this meshing, almost 80% of the total cells are located at the fluid domain which is critical part to generate the result. These unstructured cells are constructed in the majority of the tetrahedral cells combined with some prism cells and pyramidal cells. On the valve surfaces, high aspect ratio prism cells are deployed and refined at the inflation layer near the wall to capture the boundary layer gradient. According to the theoretical derivations and experimental explorations, classification of the boundary layers are viscous sub-layer ( $y^+ \leq 5$ ), buffer layer ( $5 < y^+ \leq 30$ ), log-law region ( $30 < y^+ \leq 500$ ), and outer layer (Lam & Peng, 2016). The dimensionless  $y^+$  value is defined as (Lam & Peng, 2016):

$$y^+ = \frac{u \cdot y}{\nu}$$

Where  $u$  is the friction velocity at the nearest wall;  $y$  is the distance to the nearest wall;  $\nu$  is the local kinematic viscosity of the fluid.

The first layer of cell thickness on the valve is set to be 0.05 mm and a total of 30 layer cells with a growth rate of 1.2 is modelled. With this mesh method and sizing for the inflation layers, the  $y^+$  value obtained for all cases is less than 5 and is about 1.

In the mesh sensitivity test, a total of six different meshes, M1 to M6, are used to examine the effect of the mesh size change. The mesh size is gradually coarsened from M1 to M6, and the number of cells increases with the refinement of the mesh size. In this case, M1 is the finest cells, with about 1.1 million cells, while the coarsest mesh, M6 has about 0.1 million cells.

From Table 3-4, as the total number of mesh is higher than mesh M3 (812,120 nodes), the average maximum dynamic stress is converged where the difference between the first three meshes is less than 1%. It also reveals that when meshes are coarsened, the stress values are further away from the convergence limit, where M6 gives a large relative error compared to M1. By comparing the computational time required for the first three meshes, it can be observed that, M1 requires a long computational time of up to 55 hours, while M2 and M3 are 39 hours and 33 hours respectively. Hence, in order to save computational time while maintaining promising simulation results, the M3 mesh size is chosen for the following simulations.

Table 3-4: Mesh Info

Mesh	Total no. of cells	Computation time (hrs)	Average maximum dynamic stress (MPa)
M1	1,152,230	55	41.4248
M2	903,123	39	41.4251
M3	812,120	33	41.4252
M4	569,713	15	42.5328
M5	357,687	8	44.4637
M6	119,578	5	48.3651

### 3.5 Stress Analysis (Experimental Based)

Stress calculated by strain gauges might not be the maximum as the measured vibrations on a piping span during a test reflect the conditions at the time of the test only. Besides, the best locations of strain gauge are usually based on experience, where sometimes the locations are not the points of the highest stresses. This approach gives only indirect information on the loading at the critical locations and generally leads to over conservative assessments. An important advantage of proposed method is complicated foundations involving weak joints on seams, various materials, and fracturing can be readily modelled. There is no need to guess the location of the highest stress concentration. Figure 3.8 below shows the comparison of this procedure with normal ASME Procedure.

ASME PROCEDURE	PROPOSED PROCEDURE
STRAIN GAUGES LOCATED AT A SPECIFIC POINTS BUT AWAY FROM THE STRESS CONCENTRATION REGION	ACCELEROMETERS LOCATED AT MESHED POINTS SUFFICIENT TO DEFINE THE MOTION OF THE WHOLE STRUCTURE
↓	↓
STRAIN ARE CALCULATED BY PROJECTING THEM TO THE STRESS CONCENTRATED REGION	DISPLACEMENTS ARE OBTAINED BY OPERATING DEFLECTION SHAPE (ODS) ANALYSIS WHICH GIVES THE DISPLACEMENT PATTERN OF THE TOTAL STRUCTURE
↓	↓
STRESS VALUES ARE CALCULATED FROM STRAIN AND BY GEOMETRICAL APPROXIMATIONS. LOCATION OF HIGHEST STRESS POINTS IS BY INTUITION	STRESS ARE CALCULATED USING FINITE ELEMENT ANALYSIS (FEA) BASED ON THE DISPLACEMENT INPUTS OBTAINED FROM ODS ANALYSIS. FEA DETERMINES THE MAXIMUM STRESSES; BOTH VALUES AND LOCATIONS

Figure 3-8 Comparison of ASME procedure and proposed procedure

Source of excitation for this case study are vortices. These are generated at the distance piece, at the back valve, at both of the check valves, at the connection with the main feedwater line and, to a certain degree, at pipe bends.

### 3.5.1 ANSYS Simulation-FEA

Modal analysis of the piping system is done in ANSYS simulation. The mode shapes and natural frequencies obtained can be used as a comparison to see whether resonance happened or not.



Figure 3-9 : Pipe inlet and outlet fixed support and wall inside the piping system set for Fluid-Solid interface.

### 3.6 Stress Analysis (Computational Based)

A flexible Dynamic Analysis is carried out following by the Modal Analysis. Fluid-Structure Interaction is studied using this analysis type. Flexible dynamic analysis is a technique used to determine the dynamic response of the structure under the action of any general time-dependent loads. This type of analysis can be used to determine the time-varying displacements, strains, stresses and forces in a structure as it responds to any combination of static, transient, and harmonic loads. The analysis is assumed to be linear.

From the modal analysis, the structure response can be observed when its modes are excited. The natural frequencies are also useful for calculating the correct integration time step. The time step should be small enough to resolve the motion of the structure. The solver calculates an aggregate response frequency at every time point.

Universiti Malaya

### Flow Chart of Fluid-Structure Interaction Analysis Procedures

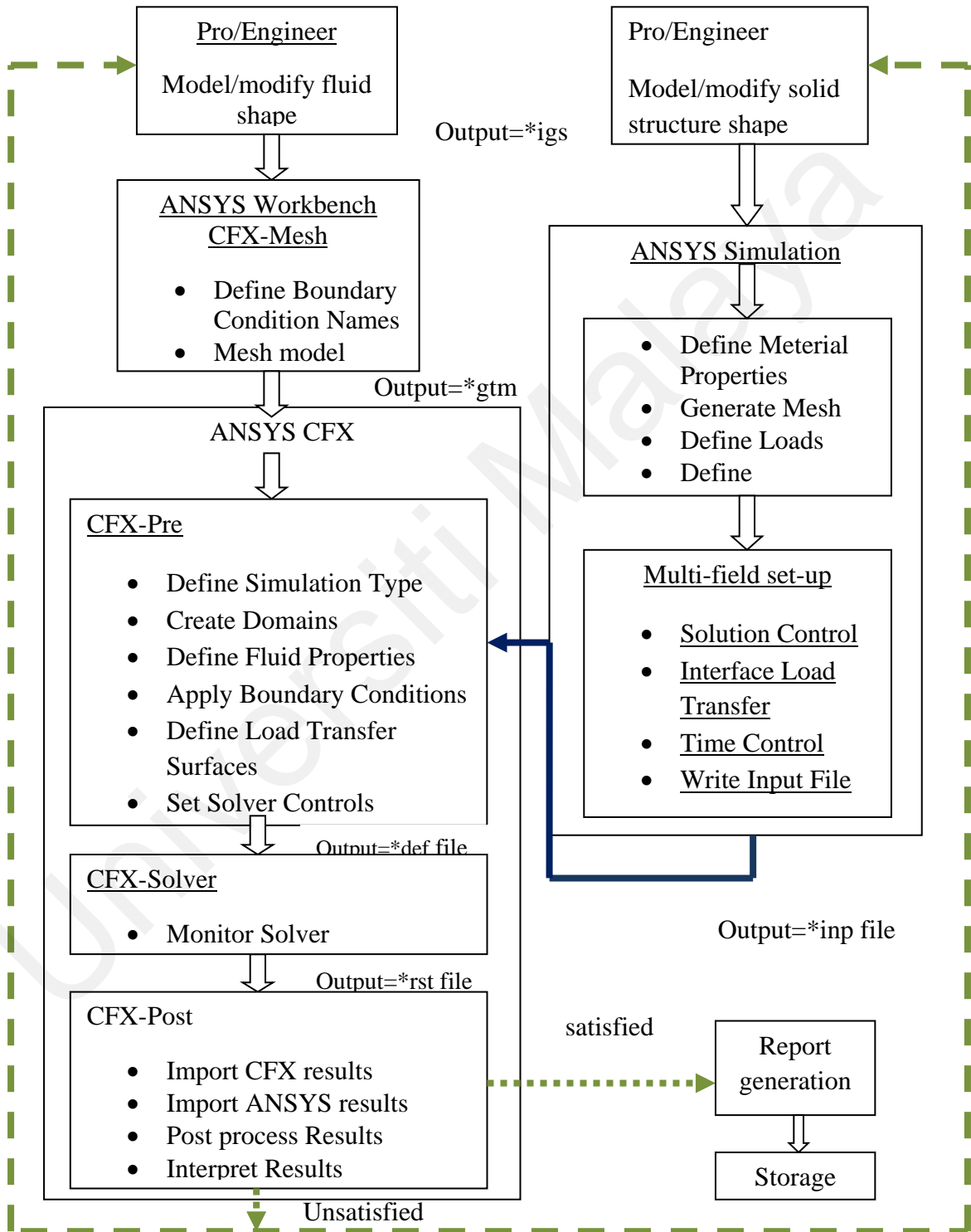


Figure 3-10 : Fluid-Structure Interaction Analysis Flow Chart

### 3.6.1 ANSYS Simulation FSI

The ANSYS simulation starts by importing the structural geometry, followed by the definition of connection and mesh generation.

ANSYS CFX provides the ability to solve the part that involves the coupling of the CFX solution field in liquid and solid domain. This coupling is referred to FSI.

1. Define domain

The various domains are defined. All the domains have the same fluid properties which are carbon dioxide at standard temperature and pressure. An assumption made which is no heat transfer in the fluid models. Mesh deformation is set to region of motion specified, which is required to allow the movement of the mesh. The turbulence model is set to SST k-omega. Besides that, the reference pressure is set to be 4500kPa and other fields are set to remain default.

2. Define boundary condition

Inlet is set to inlet boundary condition while the outlet is set to outlet boundary condition. Normal speed with flow rate velocity is set as the inlet boundary condition. For the outlet boundary condition, average static pressure is selected and -42kPa is inserted as the relative pressure. The relative pressure (-42kPa) at outlet boundary condition is referred to 4458kPa. Fluid-Structural Interaction interface are defined by using wall boundary condition. In the mesh motion, the option is set to ANSYS MultiField. The ANSYS interface number must be

correctly defined as the interface number represents the surface of the load transfer and must be matched.

The procedure to set up for only fluid region simulation in CFX analysis is the same as the above but without the complication of import the input file to set the Fluid-Structure Interaction part.

Universiti Malaysia

## **CHAPTER 4 RESULTS AND DISCUSSIONS**

### **4.1 Introduction**

In this chapter, section 4.2 is describing the 1<sup>st</sup> steps of the non-invasive measurement and evaluation procedure, which is problem identification. Then correlation of the piping system between experimental results and the FE model is described in section 4.3. Lastly, the results of the stress analysis of the piping system using experimental based approach and FSI based approach are described in section 4.4 and section 4.5 accordingly.

### **4.2 Problem identification**

It has been observed that the flow-induced vibrations may not cause excessive stresses in the main pipe but to the adjacent systems that are attached to the vibrating pipe. As a part of the non-invasive measurement and evaluation procedure, the evaluation part has been based on the allowable levels of piping vibration versus the associated frequencies criteria shown in Figure 2-1 (J. Wachel, 1981a).

From Figure 4-1, modal analysis conducted on the structure does not show any peak at the flow-induced frequencies region (5-15 Hz). All the vibration measurements on the structure are low compared to the vibration level of the pipe signifying no structural dynamics weakness. Therefore, the pipe dynamics weakness situation was evaluated along the pipe. The detailed locations are described as follows: modal analysis along the pipes shows some natural frequencies at 5-15 Hz region which might indicate the pipe dynamics

weakness for six locations named L<sub>1</sub>, L<sub>2</sub>, L<sub>3</sub>, L<sub>4</sub>, L<sub>5</sub> and L<sub>6</sub>. Cracks have been observed at the connections L<sub>3</sub>, L<sub>5</sub> and L<sub>6</sub> (between the drain valve and main pipe) and high vibrations were recorded at those locations. It was also observed that increased flow rate will increase the vibration level. As cyclic excitation (and not random vibration) generates resonance situation, it was supposed that the high vibration of the pipe was probably due to flow-induced excitation which is a stiffness-controlled situation rather than a pipe dynamics weakness. In conclusion, it was concluded that the high vibration of the pipe is probably due to the process and design problem.

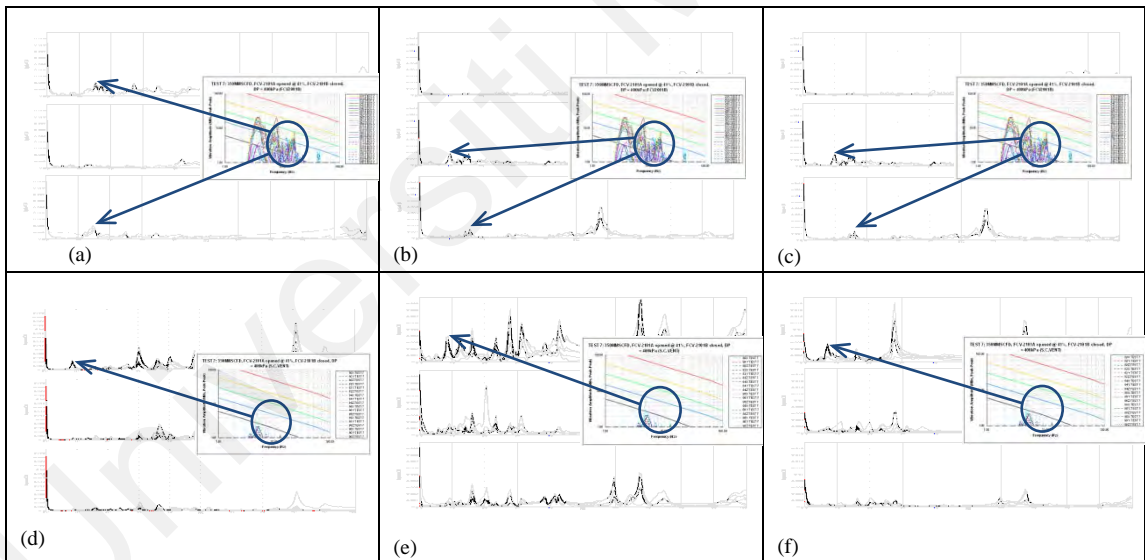


Figure 4-1 : Bump Tests on locations L<sub>1</sub>-L<sub>6</sub> are shown in (a) – (f)

The evaluation of whether or not the high vibration levels represent a problem has to be based primarily on the vibratory stresses introduced into the piping. Frequently, superficially high vibration may not cause excessive stresses in the piping but could cause

excessive stresses to piping system that is attached to the vibrating pipe. As cracks were identified at the connection between the drain valve and main pipe, vibration measurements have been carried out on the kicker line drain valve shown in Figure 4-2(a) in order to assess the vibration levels. The recorded vibrations for kicker line drain valve are shown in Figure 4-2(b) with the high vibration level dominant frequency at 47 Hz in x-axis caused mainly by the unsuitable design or selection of the drain valve.

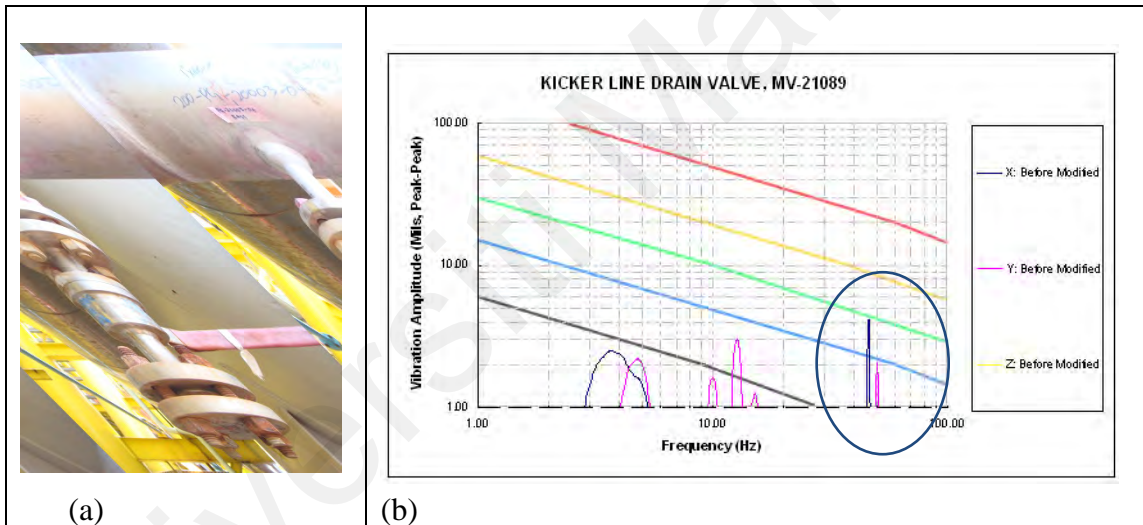


Figure 4-2 : Before modification: (a) Kicker Line Drain Valve, and (b) Valve Vibration Level vs. Frequency

The effect of the valve on the vibrations levels by vibration measurement was analysed after removing the valve as shown in Figure 4-3(a) in order to observe whether there is any excessive stress in the piping caused by the valve. It can be observed that the 47 Hz frequency component has been eliminated as shown in Figure 4-3(b).

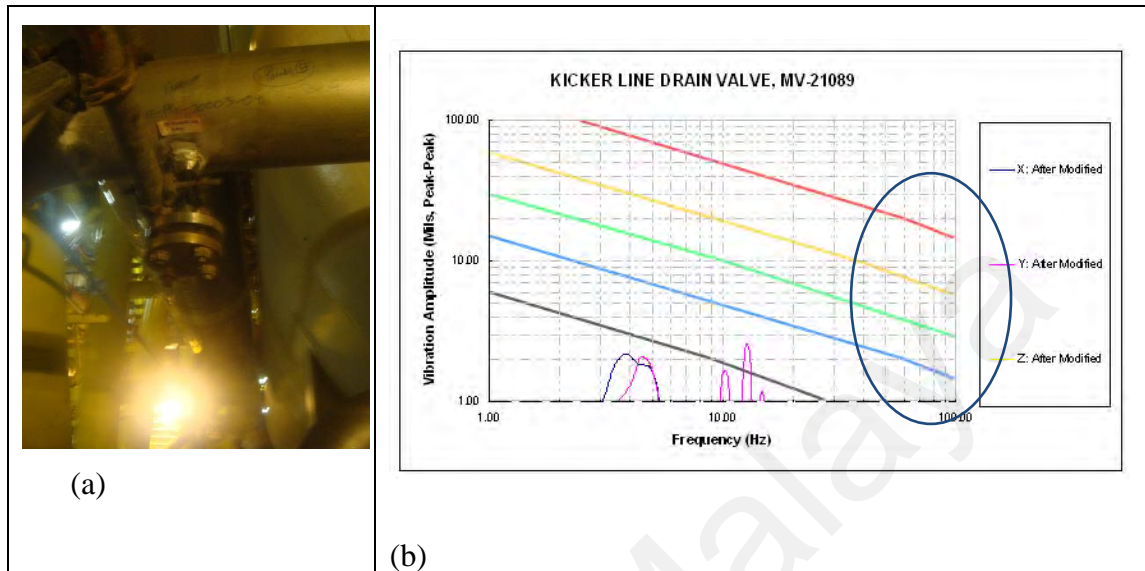


Figure 4-3 : After modification: (a) Kicker Line Drain Valve, and (b) Valve Vibration Level vs. Frequency

The cracks in the kicker drain valve have proved that the unsuitable drain valve location and improper design affect the piping system. In this case, the designed drain valves are too long and heavy; therefore, fatigue failure easily occurs for this kind of design. To evaluate the risk of apparently high vibration which may induce excessive stress to piping system that are attached to the vibrating pipe and the vibration of the pipe due to operation condition, an ODS analysis have been carried out for different testing conditions (decided based on the pipe operating conditions) as shown in Figure 4-4.

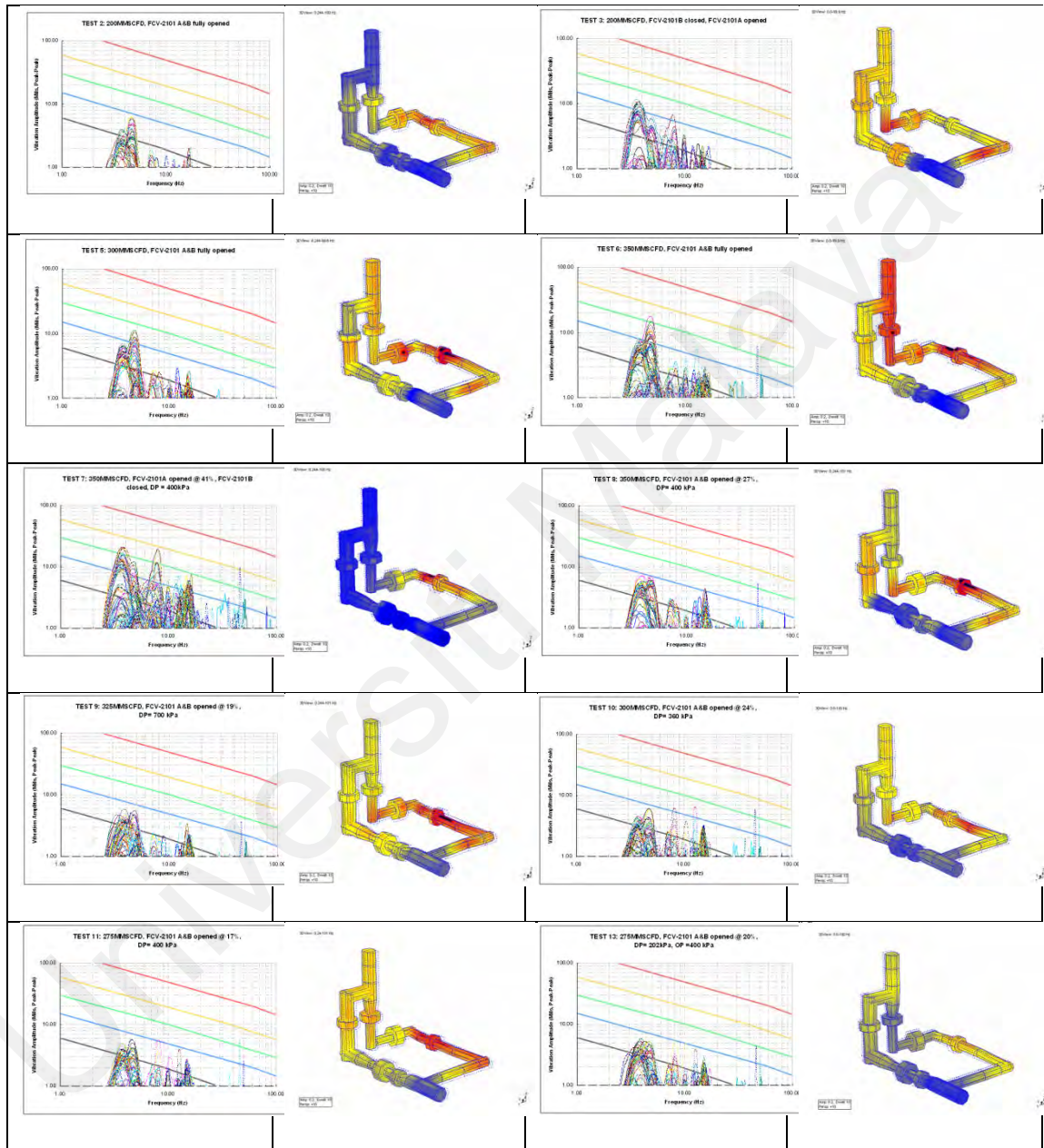


Figure 4-4 : ODS analysis for the pipe for different testing conditions

From Figure 4-4, it can be observed that the vibration amplitudes of the pipe at the measured frequencies do not overlay the danger line and therefore no failures of the pipe are anticipated. However, two additional vibration tests conducted at a maximal flow rate (350 MMSCFD) show the highest vibration levels for the pipe and a possible contribution in increasing the levels of stress to piping system that are attached to the vibrating pipe, especially when these systems which are supplied by third parties and assembled locally suffer from dynamic incompatibility. Therefore, these vibrations versus frequency criteria can serve as a good starting point in evaluating piping vibrations in screening those systems that need further analysis.

### **4.3 Correlation**

#### **4.3.1 OMA results**

The flow generated random excitation to the pipe and hence there was no issue of resonance. Resonance only occurred when cyclic excitation hitting the natural frequencies region. Therefore, ODS data was capable to reveal the mode of vibration in this case (Schwarz & Richardson, 1999). When the flow velocity is low, natural frequencies don't change much in pipeline conveying fluid (Zhai et al., 2011).

Referring to Figure 4.5, whenever piping vibration amplitudes at the measured frequencies were greater than the danger line, pipe failures occurred. When vibration level was below the design line, very few failures occurred. Therefore, these vibrations versus frequency

criteria can serve as a good starting point in evaluating piping vibrations to screen those systems that need further analysis. It can be observed from Figure 4.5 that the movement was dominated by two frequencies which are 3.60Hz and 4.56Hz. Hence, the 1<sup>st</sup> and 2<sup>nd</sup> natural frequencies were found.

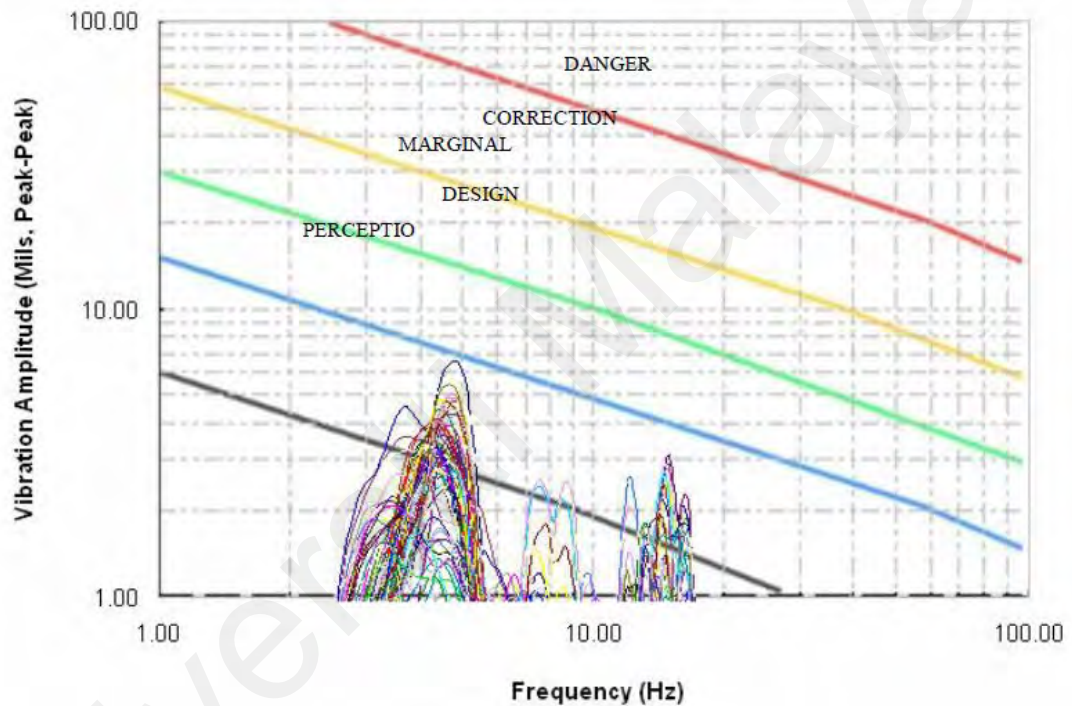


Figure 4-5 : Overlaid ODS spectra for DSS pipe which plot into the Allowable Piping Vibration Level versus Frequency

Because the mode with the lowest frequency was most easily excited by an external force, only the modes at lower frequencies were of interest in practical piping analysis. It was very difficult for modes at very high frequencies to get excited, thus they were often ignored.

Figure 4.6 and Figure 4.7 show the movement of the pipe at 3.60Hz and 4.56Hz. From observation, the movements were dominant in Y-direction at 3.60Hz and dominant in X-direction at 4.56Hz.

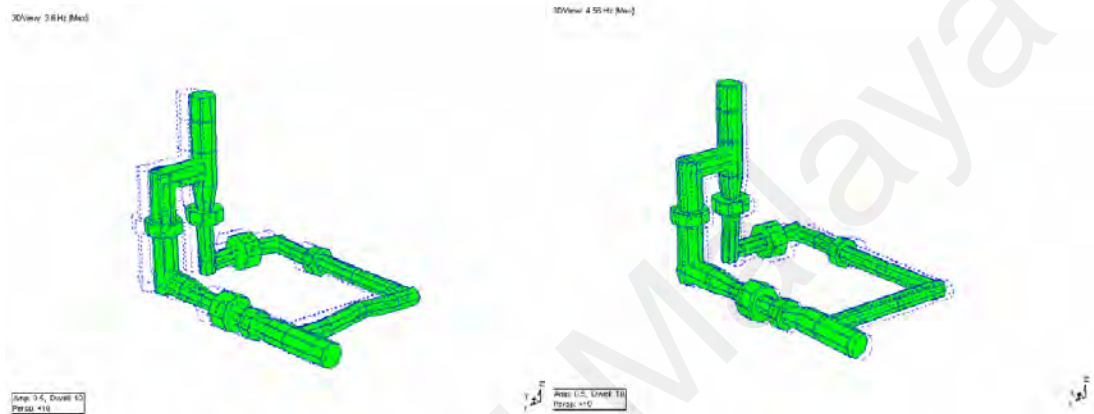


Figure 4-6 : 1<sup>st</sup> vibration mode at 3.60 Hz    Figure 4-7 : 2<sup>nd</sup> vibration mode at 4.56 Hz

FE model used in the analyses is shown in Figure 4.8. Mesh generation is an integral of the analysis process. The mesh quality can have a considerable impact on the computational analysis in term of the quality of the solution and time needed to obtain it. There are 396010 elements and 812120 nodes generated by the Finite Element (FE) software as shown in Figure 4.9. In a higher order 3-D model, 10-node element with quadratic displacement behaviour was well suited to modelling irregular meshes. As one boundary condition for the piping system, the connection with the main feed line was considered as rigid. On the other end of the system, the piping system was rigidly connected to the storage tank. The five pipe supports were also modelled in the FE, where the bottom parts of the supports are rigidly connected to the ground.

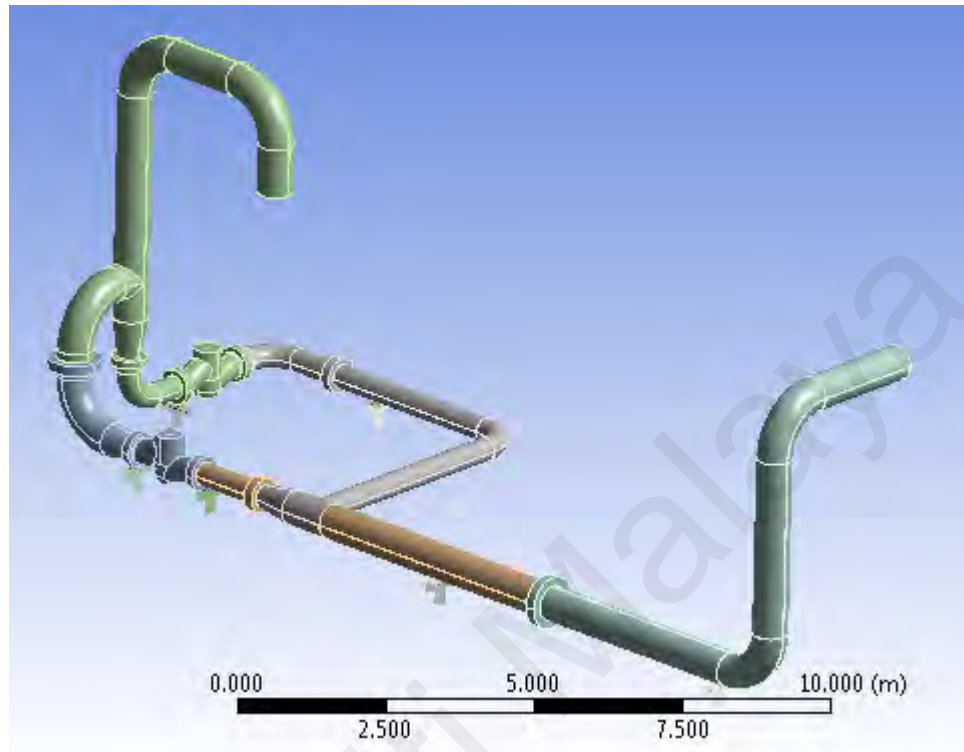


Figure 4-8 : 3D CAD Model of DSS Pipe

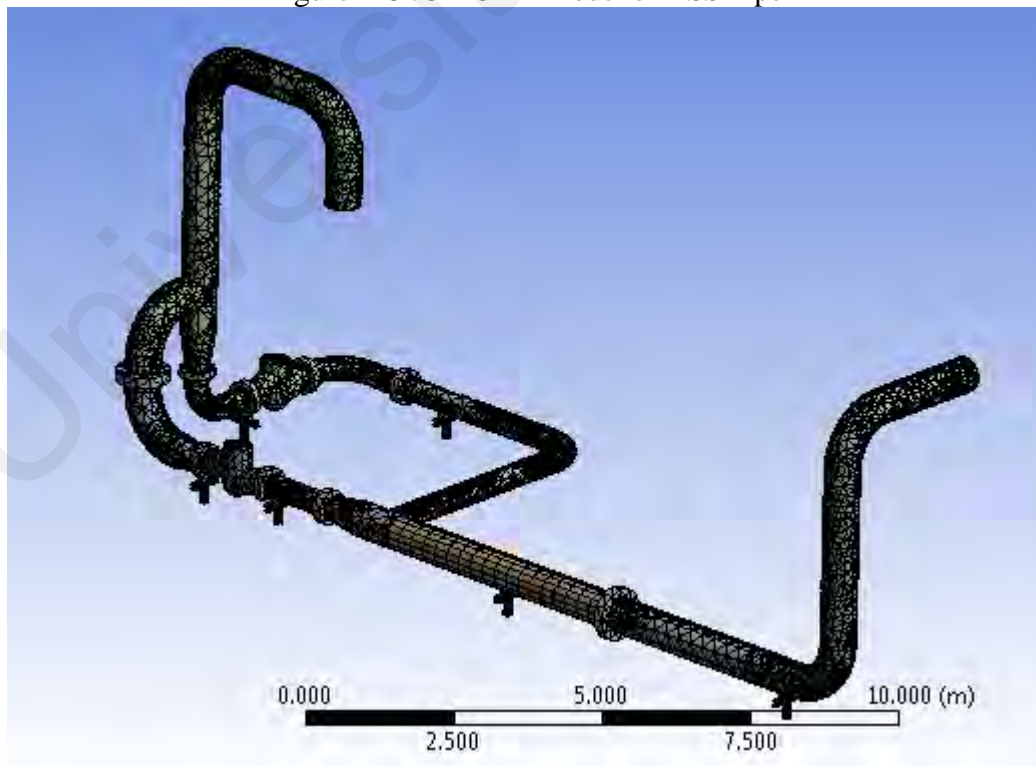


Figure 4-9 : Mesh Model of DSS Pipe

Thus, the first 2 major vibration modes and frequencies were obtained from the ODS analysis. It helped in generating a reliable model in FEA by comparing the mode shapes by visual inspection and frequency errors between FEA and ODS. A good and reliable FE model of the piping system was built based on correlation results between FEA and ODS. FE modal analysis revealed the first 2 modes of vibration at 3.84 Hz and 4.60 Hz which were dominated in X-direction and Y-direction respectively (Figure 4.10 and Figure 4.11). Therefore, the FE model was well correlated with the measurement data; further analyses such as Dynamic Stress Analysis and FSI analysis can be performed.

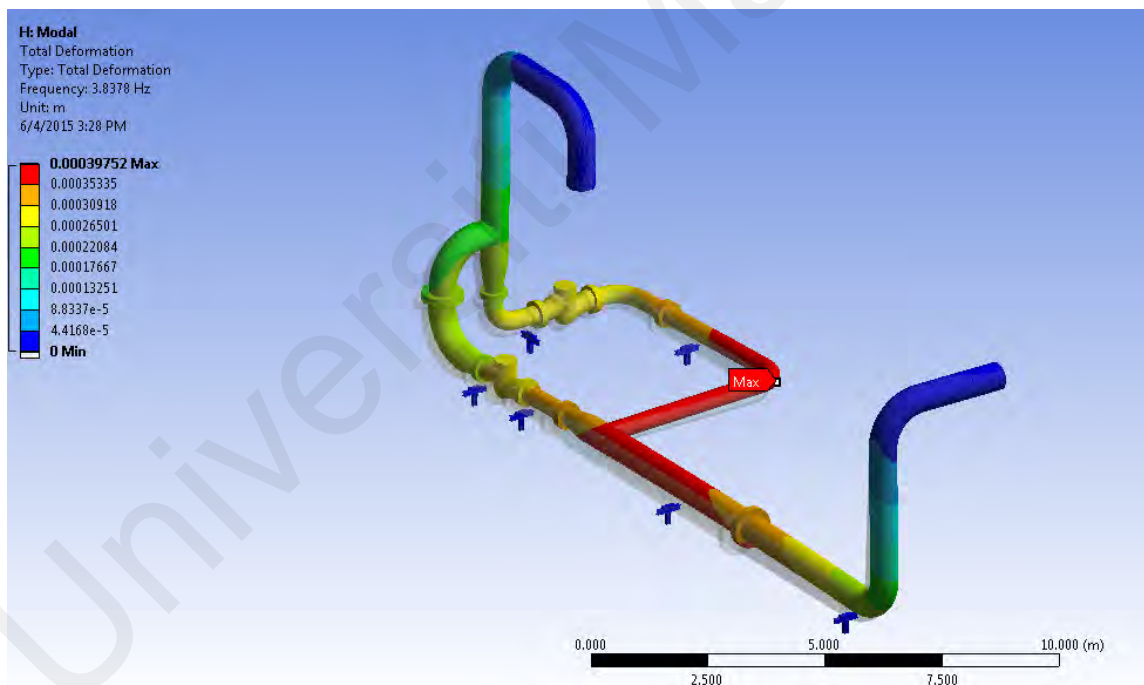


Figure 4-10 : 1st vibration mode at 3.84 Hz

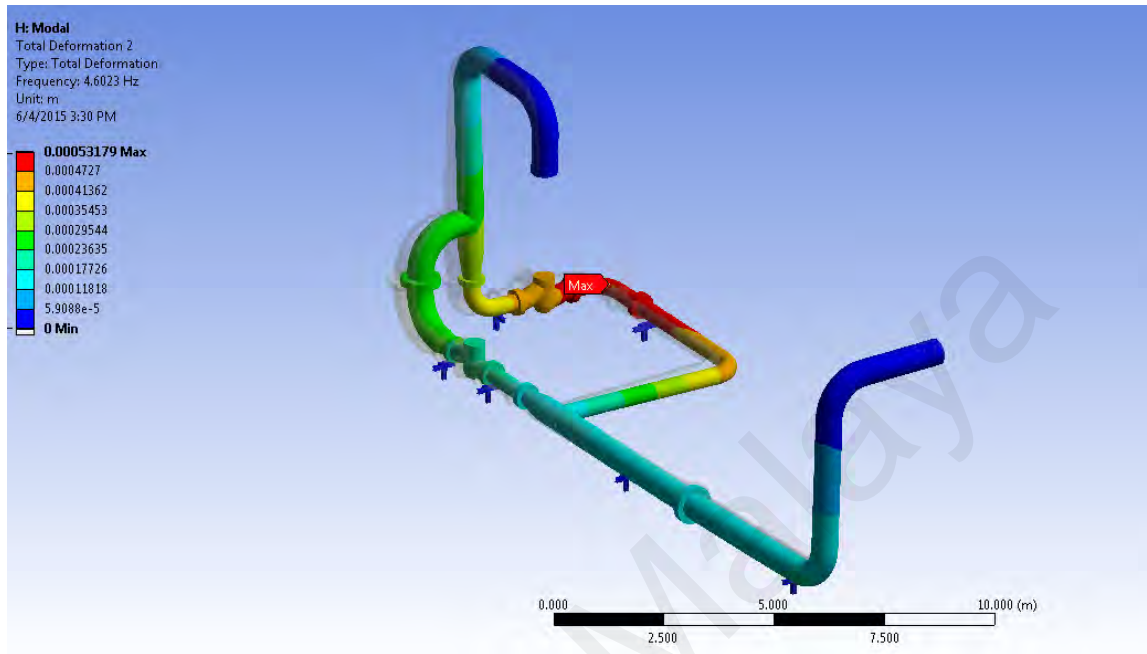


Figure 4-11: 2nd vibration mode at 4.60 Hz

#### 4.4 Stress Analysis (Experimental based)

Several sets of ODS analysis are performed on the DSS pipe under different operation conditions. For simplification purposes, this study only shows a set of ODS analysis result for partially-opened FCVs A & B @ 17% with a flow rate of 275MMSCFD and another set of ODS analysis result for fully-opened FCVs A & B with a flow rate of 300MMSCFD. Fig. 4.12 shows the overlaid ODS spectrums for the DSS pipe. The Allowable Piping Vibration Level versus Frequency for comparison is provided for preliminary screening purpose as follows reference(J. Wachel, 1981b; J. Wachel & Smith, 1991). It is observed that the movement is dominated by two frequencies which are 3.60Hz and 4.56Hz. The entire ODS spectrums are imported to FE environment for further dynamic stress analysis

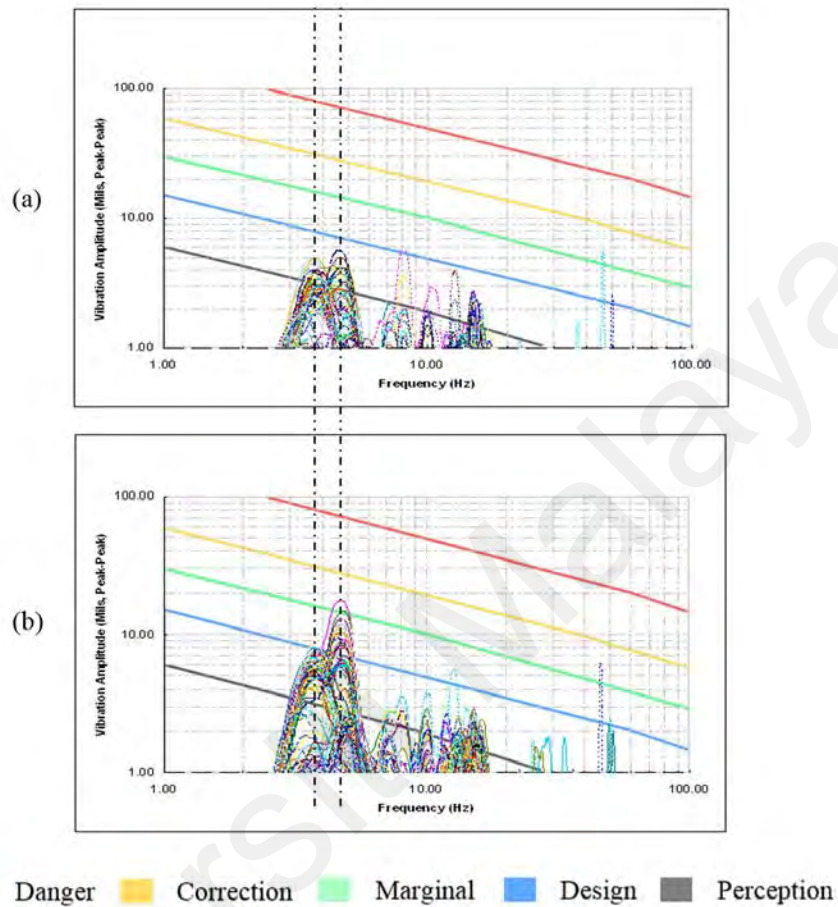


Figure 4-12 Overlaid ODS Result for DSS Pipe While Operating at (a) 275MMSCFD with partially-opened valve (b) 350MMSCFD with fully-opened valve

Displacements are obtained by Operating Deflection Shape (ODS) analysis which gives the displacement pattern of the total structure. Dynamics Stress is calculated using Finite Element Analysis (FEA) based on the values in X, Y and Z directions for 1<sup>st</sup> and 2<sup>nd</sup> vibration modes obtained from ODS analysis. Only the first 2 modes are considered as the 2 mode dominant the vibration. Then the stress obtained for the 2 modes is added up based on the principle of superposition.

Figure 4.13(a) shows the dynamics stress results obtained from the first 2 vibration modes of 275MMSCFD (partially-opened valve). For dynamic stress at 3.60Hz, it is observed the maximum stress register at 28.24MPa and located at location labelled I as shown in Figure 4.13(a). For dynamic stress at 4.56Hz, it is observed the maximum stress register at 47.94MPa and located at location labelled II as shown in Figure 4.13(a).

Figure 4.13(b) shows the dynamics stresses obtain from the first 2 vibration modes of 350MMSCFD (fully-opened valve). For dynamic stress at 3.60Hz, it is observed the maximum stress register at 35.58MPa and located at the location labelled III as shown in Figure 4.13(b). For dynamic stress at 4.56Hz, it is observed the maximum stress register at 78.58MPa and located at location labelled IV as shown in Figure 4.13(b).

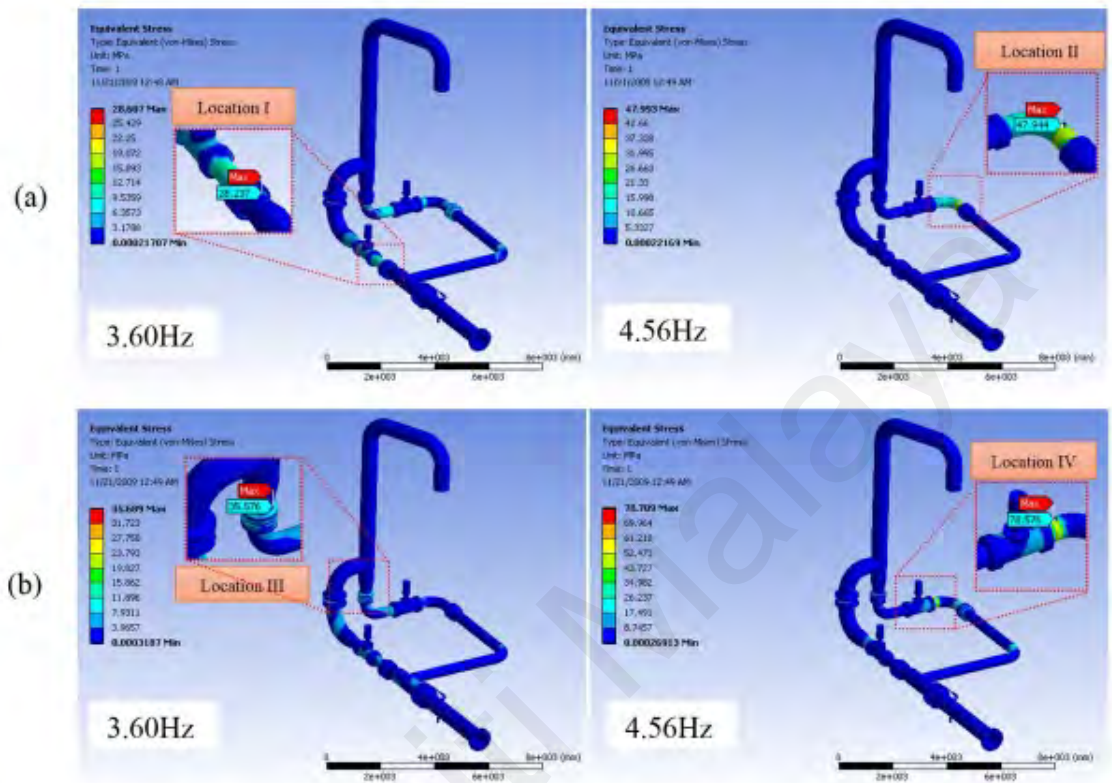


Figure 4-13 Dynamics Stress of piping operating at 3.60Hz and 4.56Hz respectively for various flow rates: (a) 275MMSCFD (partially-opened valve) (b) 350MMSCFD (fully-opened valve)

Table 4-1 shows the high-stress location for each vibration mode. The summation of the stresses for mode 1 and mode 2 at the same location will give the total stress values. Overall, the total stress for all the locations is under the pipe stress allowable limit (93.8MPa) for indefinite lifecycle.

Table 4-1 Summary of Dynamic Stress Level for various flow rates: (a) 275MMSCFD (partially-opened valve) (b) 350MMSCFD (fully-opened valve)

Condition	Location	Stress Level		Total Stress (Mode 1 + Mode 2)
		Mode 1 (3.60Hz)	Mode 2 (4.56Hz)	
275mmscfd (partially-opened valve)	I	28.24MPa (Max. for Mode 1)	13.18MPa	41.42MPa
	II	3.88MPa	47.94MPa (Max. for Mode 2)	51.82MPa
350mmscfd (fully-opened valve)	III	35.58MPa (Max. for Mode 1)	32.22MPa	67.80MPa
	IV	8.82MPa	78.58MPa (Max. for Mode 2)	87.40MPa

#### 4.5 Stress Analysis (FSI based)

For partially-opened FCVs A & B @ 17% with a flow rate of 275MMSCFD and fully-opened FCVs A & B with a flow rate of 300MMSCFD, operating parameters of the fluid such as Operating Pressure (OP), Differential Pressure (DP) and flow rate were applied in ANSYS CFX, which coupled with ANSYS mechanical to conduct FSI analysis.

Figure 4.14 shows the dynamic stress results obtain from FSI analysis of case 275MMSCFD (partially-opened valve). Maximum dynamic stress at the location I and location II in Figure 4.13 is collected and recorded at Table 4-2. Figure 4.15 shows the dynamic stress results obtain from FSI analysis of case 350MMSCFD (fully-opened valve). Maximum dynamic stress at location III and location IV in Figure 4.13 is collected and recorded at Table 4-2.

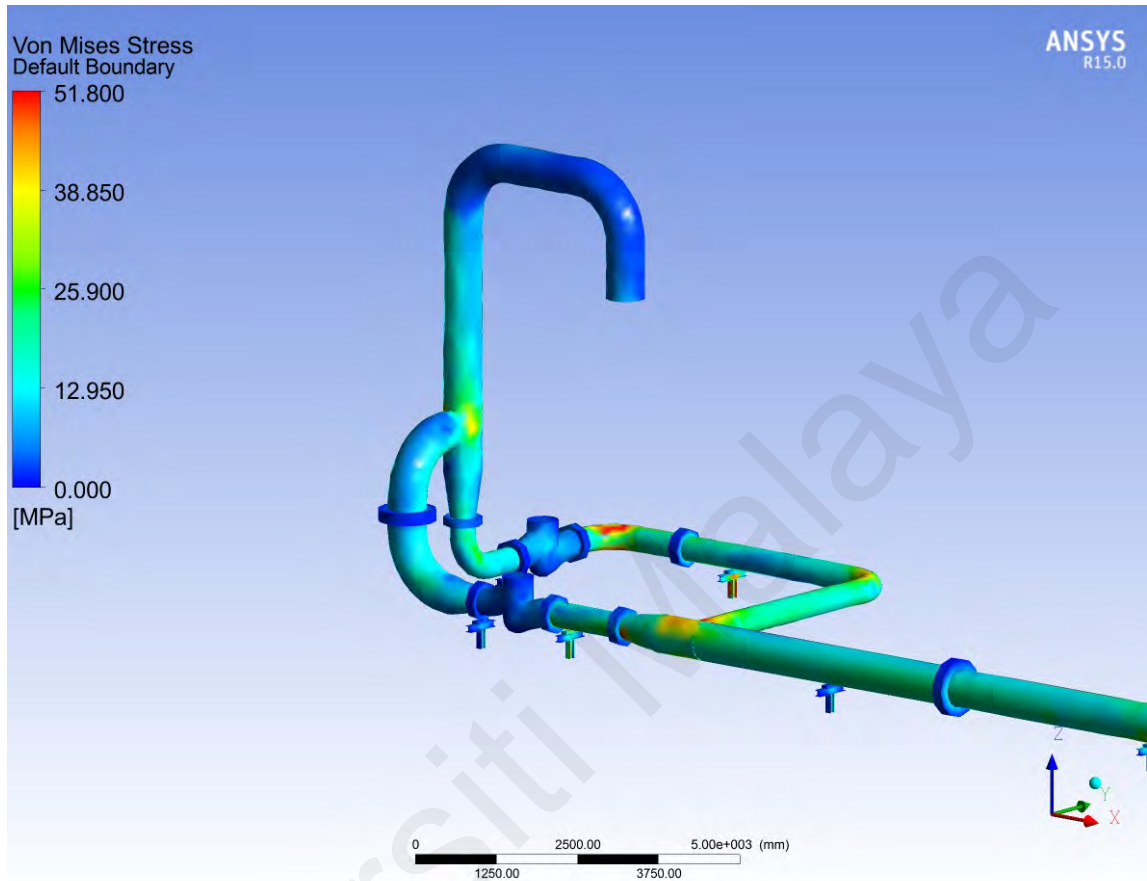


Figure 4-14 Dynamics Stress from FSI analysis of piping operating at 275MMSCFD (partially-opened valve)

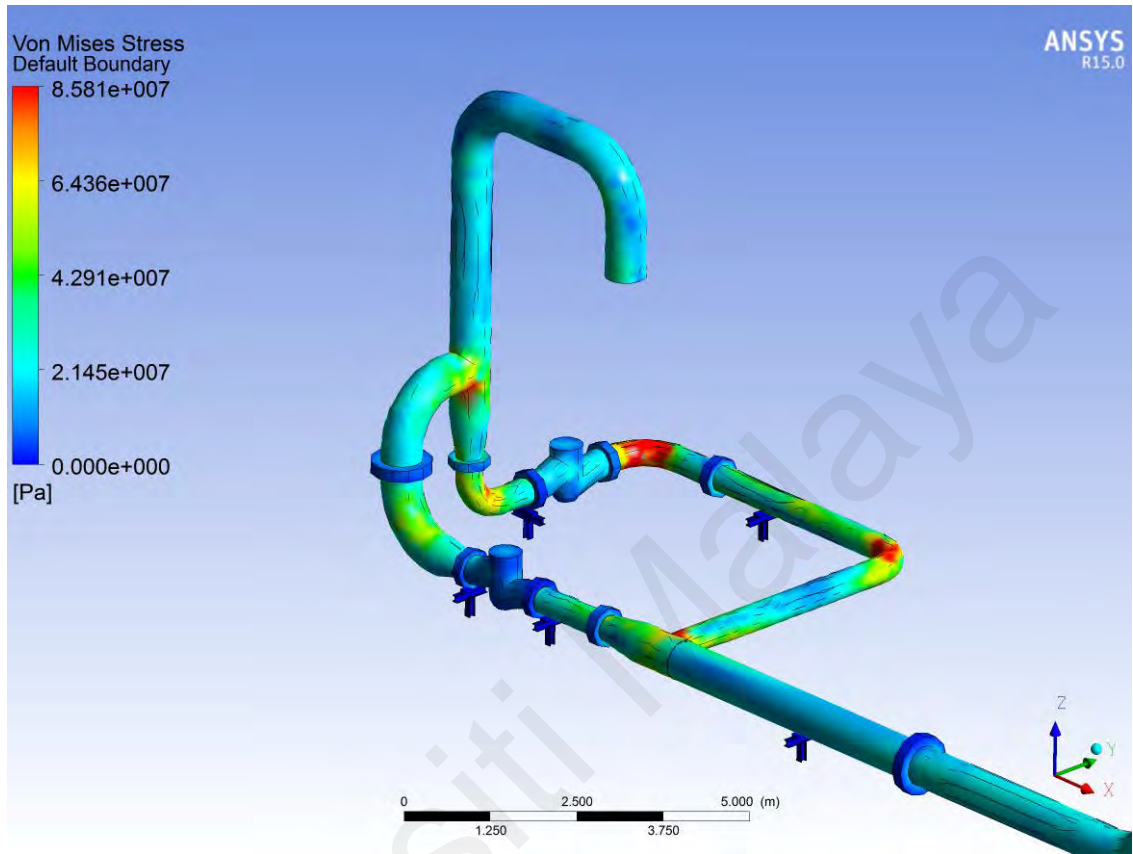


Figure 4-15 Dynamics Stress from FSI analysis of piping operating at 350MMSCFD (fully-opened valve)

Table 4-2 Summary of Dynamic Stress Level for various flow rates from ODS based and FSI based: (a) 275MMSCFD (partially-opened valve) (b) 350MMSCFD (fully-opened valve)

Condition	Location	Total Stress (Experimental based)	Total Stress (FSI based)	Differences (%)
275MMSCFD (partially-opened valve)	I	41.42MPa	41.425MPa	0.01
	II	51.82MPa	51.800MPa	0.04
350MMSCFD (fully-opened valve)	III	67.80MPa	69.58MPa	2.62
	IV	87.40MPa	85.81MPa	1.82

From the result in Table 4-2, dynamic stress obtained from ODS based and FSI analysis based is agreed with each other from the aspect of locations and values (less than 3% differences).

Universiti Malaya

## **CHAPTER 5 CONCLUSIONS**

### **5.1 Conclusion**

The outcome of an industrial case study that involved condition monitoring of a piping system that showed signs of excess fatigue due to flow-induced vibration is presented. Due to operational requirement, a novel non-destructive assessment stratagem was adopted using different vibration analysis techniques - such as EMA and ODS - and complemented by visual inspection.

Preliminary inspection with visual inspection was conducted and cracks were found at the connection between the drain valve and the main pipe. Then, vibration measurements had been carried out to obtain the vibration levels of the piping system. The results were then fed into a screening tool based on vibration level versus frequency criteria as shown in Figure 4-4. There were some conditions where vibration levels exceed the marginal line and approach to correction line. Therefore, stress analysis needed to be carried out to rule out excessive stress that might cause fatigue failure.

In order to conduct stress analysis, a finite element 3D model of the piping system had been created. Dynamic characteristics such as mode shapes and natural frequencies of the piping system were obtained through ODS analysis. Dynamic characteristic of the finite element model was obtained by conducting a computational modal analysis. Then the finite element model was correlated and verified using experimental and computational results.

Next, the displacements of the piping system during operating condition obtained from ODS analysis is used as input for the dynamic stress analysis. As a result of dynamic stress analysis, maximum dynamic stress is obtained for various flow rates: (a) 275MMSCFD (partially-opened valve) (b) 350MMSCFD (fully-opened valve). The maximum dynamic stress was obtained by summation of stress for 2 modes based on the principle of superposition. The summation of the stresses for mode 1 and mode 2 at the same location will give the total stress values. Overall, the total stress for all the locations is under the pipe stress allowable limit (93.8MPa) for indefinite lifecycle.

Then, stress analysis using coupled fluid-structure interaction computational mechanics for flow-induced vibration piping system is conducted. Operating parameters of the fluid such as Operating Pressure (OP), Differential Pressure (DP) and flow rate were applied in ANSYS CFX, which coupled with ANSYS mechanical to conduct FSI analysis. The location and value (less than 3% differences) of dynamic stress agreed with experimental based stress evaluation approach.

## 5.2 Future recommendation

The level of the vibration-induced stress is not very high at any of the studied output points. However, further proofing that the vibration does not increase the risk of fatigue failure, in this case, would require further processing of the results, completed with information about the hoop stress variation, nominal stress level and the material data. It was deduced that the main factors that increase the uncertainty of the results are:

- The fact that no measurement contains the exact ODS as they were at the time of measurement. This issue is difficult to solve since it is strongly dictated by the available and feasible measurement instruments.
- The fact the ODS were identified only from the low-frequency range of 4.38 Hz to 21.06 Hz
- Application of the superposition principle to the stresses of the individual ODS. This simplifies the computation process. It is reasonable to assume that the results are not affected too much by this procedure.
- Conduct Structural Design Modification (SDM) in the future to rectify any problem come across.
- Able to find the optimized operating condition for the piping system without failure.

## REFERENCE

- Agency, O. N. E. (2006). *Nuclear Power Plant Operating Experiences from the IAEA/NEA Incident Reporting System 2002-2005*. Retrieved from
- Ashrafizadeh, H., Karimi, M., & Ashrafizadeh, F. (2013). Failure analysis of a high pressure natural gas pipe under split tee by computer simulations and metallurgical assessment. *Engineering Failure Analysis*, 32(0), 188-201. doi:<http://dx.doi.org/10.1016/j.engfailanal.2013.03.013>
- ASME B&PV Code-III. (2007). Rules for Construction of Nuclear Power Plant Components. In *Boiler & Pressure Vessel Code, Section-III, ASME, New York, NY*.
- Bai, B., Zhang, C., Lou, X., Lin, Y., Lin, H., Tong, Z., . . . Yang, W. (2017). Failure analysis of nozzle zone before valve of negative pressure chamber from main pipe coolant system in nuclear power plant. *Engineering Failure Analysis*, 82, 783-790.
- Blevins, R. D. (1990). *Flow-induced vibration* (2nd ed.). New York: Van Nostrand Reinhold.
- Chen, S.-S. (1987). *Flow-induced vibration of circular cylindrical structures* (Vol. 1). Washington, DC: Hemisphere Publishing Corp.
- Dai, H. L., Wang, L., Qian, Q., & Gan, J. (2012). *Vibration analysis of three-dimensional pipes conveying fluid with consideration of steady combined force by transfer matrix method*. *Applied Mathematics and Computation*, (219, 5).
- De, C., Zhen-Qiang, Y., Ya-Bo, X., & Hong, S. (2014). Numerical study on seismic response of the reactor coolant pump in Advanced Passive Pressurized Water Reactor. *Nuclear Engineering and Design*, 278, 39-49.
- Devriendt, C., Steenackers, G., De Sitter, G., & Guillaume, P. (2010). From operating deflection shapes towards mode shapes using transmissibility measurements. *Mechanical Systems and Signal Processing*, 24(3), 665-677. doi:DOI: 10.1016/j.ymsp.2009.10.018
- Dilena, M., & Morassi, A. (2004). Experimental modal analysis of steel concrete composite beams with partially damaged connection. *Journal of Vibration and Control*, 10(6), 897-913. Retrieved from <http://jvc.sagepub.com/content/10/6/897.full.pdf>
- Dong, L., Ibrahim, Z., Hangzhou, Y., & Ismail, Z. (2013). Use of Tapered Optical Fiber Sensors in Study of the Hydration Process of Cement Paste. *Sensors Journal, IEEE*, 13(9), 3415-3420. doi:10.1109/JSEN.2013.2263224

- Enz, S., & Thomsen, J. J. (2011). Predicting phase shift effects for vibrating fluid-conveying pipes due to Coriolis forces and fluid pulsation. *Journal of Sound and Vibration*, 330(21), 5096-5113. doi:<http://dx.doi.org/10.1016/j.jsv.2011.05.022>
- Ewins, D. J. (2000). *Modal testing: theory, practice and application* (Vol. 2): Research studies press Baldock.
- Fayyadh, M. M., Razak, H. A., & Ismail, Z. (2011). Combined modal parameters-based index for damage identification in a beamlike structure: theoretical development and verification. *Archives of Civil and Mechanical Engineering*, 11(3), 587-609. doi:[http://dx.doi.org/10.1016/S1644-9665\(12\)60103-4](http://dx.doi.org/10.1016/S1644-9665(12)60103-4)
- Ferras, D., Manso, P. A., Schleiss, A. J., & Covas, D. I. (2017). Fluid-structure interaction in straight pipelines with different anchoring conditions. *Journal of Sound and Vibration*, 394, 348-365.
- Fomin, V., Kostarev, V., & Reinsch, K. (2001). *Elimination of Chernobyl NPP unit 3 power output limitation associated with high main steam piping flow induced vibration*. Paper presented at the Proceedings of the 16th International Conference on Structural Mechanics in Reactor Technology, Washington, DC, USA.
- Gamble, R., & Tagart Jr, S. (1991). A method to assign failure rates for piping reliability assessments. In W. H. Bamford (Ed.), *Fatigue, fracture, and risk 1991* (Vol. 215, pp. 3-12). New York: ASME.
- Garrison, W. G. (1988). Major fires and explosions analyzed for 30-year period. *Hydrocarbon processing*, 67(9), 115-118.
- Geng, Y., Ren, F., & Hua, C. (2012). An auxiliary measuring technology of wet gas flow based on the vibration signals of the pipe. *Flow Measurement and Instrumentation*, 27(0), 113-119. doi:<http://dx.doi.org/10.1016/j.flowmeasinst.2012.04.010>
- Giannopapa, C., & Papadakis, G. (2004). *A new formulation for solids suitable for a unified solution method for fluid-structure interaction problems*. Paper presented at the ASME/JSME 2004 Pressure Vessels and Piping Conference.
- Hansson, P.-A., & Sandberg, G. (2001). Dynamic finite element analysis of fluid-filled pipes. *Computer Methods in Applied Mechanics and Engineering*, 190(24-25), 3111-3120. Retrieved from <http://www.sciencedirect.com/science/article/B6V29-42HFP5W-9/2/27fd06594c78632e5cfa7f32245008de>
- Huang, D., Zhao, Y., & Chen, Y. (2017). Safety evaluation of a collapsed turbine wind on the buried pipeline. *Engineering Failure Analysis*, 82, 47-55.

- Ismail, Z. (2012). Application of residuals from regression of experimental mode shapes to locate multiple crack damage in a simply supported reinforced concrete beam. *Measurement*, 45(6), 1455-1461.  
doi:<http://dx.doi.org/10.1016/j.measurement.2012.03.006>
- Ismail, Z. (2012). Finite element model updating of reinforced concrete beams with honeycomb damage. *Archives of Civil Engineering*, 58(2), 135-151.  
doi:10.2478/v.10169-012-0008-x
- Ismail, Z., Doostdar, S., & Harun, Z. (2012). Factors influencing the implementation of a safety management system for construction sites. *Safety Science*, 50(3), 418-423. doi:<http://dx.doi.org/10.1016/j.ssci.2011.10.001>
- Ismail, Z., Ibrahim, Z., Ong, A., & Rahman, A. (2011). Approach to reduce the limitations of modal identification in damage detection using limited field data for nondestructive structural health monitoring of a cable-stayed concrete bridge. *Journal of Bridge Engineering*, 17(6), 867-875.
- Ismail, Z., & Karim, R. (2013). Some technical aspects of spills in the transportation of petroleum materials by tankers. *Safety Science*, 51(1), 202-208.  
doi:<http://dx.doi.org/10.1016/j.ssci.2012.06.024>
- Ismail, Z., & Ong, Z. C. (2012). Honeycomb damage detection in a reinforced concrete beam using frequency mode shape regression. *Measurement*, 45(5), 950-959.  
doi:10.1016/j.measurement.2012.01.049
- Ismail, Z., Ramli, A. H., & Somarin, S. D. (2012). Lessons Learned from Accidents in Downstream Petroleum Product Processing and Handling. *Oil Gas-European Magazine*, 38(3), 157-162.
- Jones, W., & Launder, B. (1972). The prediction of laminarization with a two-equation model of turbulence. *International Journal of Heat and Mass Transfer*, 15(2), 301-314.
- Keramat, A., Tijsseling, A., Hou, Q., & Ahmadi, A. (2012). Fluid–structure interaction with pipe-wall viscoelasticity during water hammer. *Journal of Fluids and Structures*, 28, 434-455.
- Koo, G. H., & Park, Y. S. (1996). Vibration analysis of a 3-dimensional piping system conveying fluid by wave approach. *International Journal of Pressure Vessels and Piping*, 67(3), 249-256. Retrieved from  
<http://www.sciencedirect.com/science/article/B6V3N-3V3V0K6-3/2/0ed44ed156115e8e0448c3b12128d130>

- Kustu, O., & Scholl, R. (1980). *Research Needs for Resolving the Significant Problems of Light-Water Reactor Piping Systems*. Paper presented at the Proceedings of ANS/EMS Topical Meeting—Thermal Reactor Safety, Knoxville, TN, USA.
- Lam, H., & Peng, H. (2016). Study of wake characteristics of a vertical axis wind turbine by two-and three-dimensional computational fluid dynamics simulations. *Renewable Energy*, *90*, 386-398.
- Latimer, G., Marcum, W. R., Howard, T. K., Jones, W., Phillips, A. M., Woolstenhulme, N., . . . Moussaoui, M. (2018). On the flow induced vibration of an externally excited nuclear reactor experiment. *Nuclear Engineering and Design*, *335*, 1-17.
- Lin, M.-B., Gao, K., Wang, C.-J., & Volinsky, A. A. (2012, 10//). *Failure analysis of the oil transport spiral welded pipe*. *Engineering Failure Analysis*, (25, 0).
- Lin, W., Qiao, N., & Yuying, H. (2007). Dynamical behaviors of a fluid-conveying curved pipe subjected to motion constraints and harmonic excitation. *Journal of Sound and Vibration*, *306*(3-5), 955-967.  
doi:<http://dx.doi.org/10.1016/j.jsv.2007.06.046>
- Ling, H.-y., Lau, K.-t., Cheng, L., & Jin, W. (2006). Viability of using an embedded FBG sensor in a composite structure for dynamic strain measurement. *Measurement*, *39*(4), 328-334.  
doi:<http://dx.doi.org/10.1016/j.measurement.2005.11.011>
- Liu, G., & Li, Y. (2011). Vibration analysis of liquid-filled pipelines with elastic constraints. *Journal of Sound and Vibration*, *330*(13), 3166-3181.
- Liu, Z., & Kleiner, Y. (2013). State of the art review of inspection technologies for condition assessment of water pipes. *Measurement*, *46*(1), 1-15.  
doi:<http://dx.doi.org/10.1016/j.measurement.2012.05.032>
- Lou, D., Ibrahim, Z., & Ismail, Z. (2011). Monitoring of Curing Temperature of Early-Age Cement Paste Using Biconical Tapered Fiber Sensor. *Advanced Materials Research*, *250*, 3549-3553.
- Luo, D., Ibrahim, Z., Ismail, Z., & Xu, B. (2013). Optimization of the Geometries of Biconical Tapered Fiber Sensors for Monitoring the Early-Age Curing Temperatures of Concrete Specimens. *Computer-Aided Civil and Infrastructure Engineering*, *28*(7), 531-541.
- Luo, D., Ismail, Z., & Ibrahim, Z. (2013). Added advantages in using a fiber Bragg grating sensor in the determination of early age setting time for cement pastes. *Measurement*, *46*(10), 4313-4320.  
doi:<http://dx.doi.org/10.1016/j.measurement.2013.06.036>

- Lynch, J. (1991). *Impedance-coupled valve and fluid system instability*. Paper presented at the Proceedings of the International Topical Meeting Advances in Mathematics, Computations, and Reactor Physics, Pittsburgh, PA, USA.
- Majid, Z. A., Mohsin, R., & Yusof, M. Z. (2012). Experimental and computational failure analysis of natural gas pipe. *Engineering Failure Analysis*, 19(0), 32-42. doi:<http://dx.doi.org/10.1016/j.engfailanal.2011.09.004>
- Makowski, P. L., Morawski, R. Z., Michalik, Ł., & Domanski, A. W. (2011). An efficient algorithm for processing data from a multi-point sensor of vibrations. *Measurement*, 44(10), 2060-2067. doi:<http://dx.doi.org/10.1016/j.measurement.2011.08.002>
- Marscher, W. D., & Jen, C.-W. (1999). *Use of operating deflection and mode shapes for machinery diagnostics*. Paper presented at the Proceedings of 17th International Modal Analysis conference, Kissimmee, Florida.
- McHargue, P. L., & Richardson, M. H. (1993). *Operating detection shapes from time versus frequency domain measurements*. Paper presented at the IMAC-XI The 11th International Modal Analysis Conference and Exposition, Kissimmee, Florida.
- Menter, F. R. (1994). Two-equation eddy-viscosity turbulence models for engineering applications. *AIAA journal*, 32(8), 1598-1605.
- Miller, H. L. (2001). *Piping Vibrations Involving Control Valves*. Paper presented at the Internatoinal Joint Generation Conference and Exposition ASME International-Power Division. New Orleans, LA: 2001.
- Mohanty, P., & Rixen, D. J. (2004). A modified Ibrahim time domain algorithm for operational modal analysis including harmonic excitation. *Journal of Sound and Vibration*, 275(1-2), 375-390. doi:<http://dx.doi.org/10.1016/j.jsv.2003.06.030>
- Mohsin, R., Majid, Z. A., & Yusof, M. Z. (2013). Multiple failures of API 5L X42 natural gas pipe: Experimental and computational analysis. *Engineering Failure Analysis*, 34(0), 10-23. doi:<http://dx.doi.org/10.1016/j.engfailanal.2013.07.007>
- Monajemi, H., Razak, H. A., & Ismail, Z. (2013). Damage detection in frame structures using damage locating vectors. *Measurement*, 46(9), 3541-3548. doi:<http://dx.doi.org/10.1016/j.measurement.2013.07.002>
- Noda, M., Suzuki, M., Maekawa, A., Sasaki, T., Suyama, T., & Fujita, K. (2006). *Methods of Evaluating Vibration Induced Stress of Small-Bore Piping*. Paper presented at the ASME 2006 Pressure Vessels and Piping/ICPVT-11 Conference.

- Olson, D. E. (1985). Piping Vibration Experience in Power Plants. *American Society of Mechanical Engineers, Pressure Vessel and Piping Technology--1985: a Decade of Progress*, 689-705.
- Olson, D. E. (2002). *Pipe Vibration Testing and Analysis*. Paper presented at the Companion Guide to the ASME Boiler & Pressure Vessel Code, New York.
- OM-S/G-2003, A. (2004). Standards and Guides for Operation and Maintenance of Nuclear Power Plants,. In *Part 3: "Requirements for Preoperational and Initial Start-up Vibration Testing of Nuclear Power Plant Piping Systems,"*. New York: The American Society of Mechanical Engineers.
- Ong, Z. C., Rahman, A. G. A., & Ismail, Z. (2014). Determination of Damage Severity on Rotor Shaft Due to Crack Using Damage Index Derived from Experimental Modal Data. *Experimental techniques*, 38(5), 18-30. doi:10.1111/j.1747-1567.2012.00823.x
- Panda, L. N., & Kar, R. C. (2008). Nonlinear dynamics of a pipe conveying pulsating fluid with combination, principal parametric and internal resonances. *Journal of Sound and Vibration*, 309(3–5), 375-406.  
doi:<http://dx.doi.org/10.1016/j.jsv.2007.05.023>
- Pascual R, Golinval JC, & M, R. (1999). *On-line damage assessment using operating detection shapes*. Paper presented at the IMAC XVII - 17th International Modal Analysis Conference, Kissimmee, Florida.
- Peeters, B., & De Roeck, G. (2001). Stochastic system identification for operational modal analysis: a review. *Journal of Dynamic Systems, Measurement, and Control*, 123(4), 659-667.
- Plaut, R. H. (2006). Postbuckling and vibration of end-supported elastica pipes conveying fluid and columns under follower loads. *Journal of Sound and Vibration*, 289(1–2), 264-277. doi:<http://dx.doi.org/10.1016/j.jsv.2005.02.032>
- Rahman, A. G. A., Chao, O. Z., & Ismail, Z. (2010). *Effectiveness of Impact-Synchronous Time Averaging in determination of dynamic characteristics of a rotor dynamic system*. doi: DOI: 10.1016/j.measurement.2010.09.005. Measurement, (In Press, Corrected Proof).
- Rahman, A. G. A., Ismail, Z., Noroozi, S., & Chao, O. Z. (2013). *Study of open crack in rotor shaft using changes in frequency response function phase*. *International Journal of Damage Mechanics*, (22, 6).
- Rahman, A. G. A., Ong, Z. C., & Ismail, Z. (2011). Enhancement of coherence functions using time signals in Modal Analysis. *Measurement*, 44(10), 2112-2123.  
doi:<http://dx.doi.org/10.1016/j.measurement.2011.08.003>

- Rao, S. S., & Yap, F. F. (2011). *Mechanical vibrations* (Vol. 5). New Jersey: Prentice Hall.
- Rouabeh, K., Schmitt, C., Elaoud, S., Hadj-Taïeb, E., & Pluvinage, G. (2012). Failure of grey cast iron water pipe due to resonance phenomenon. *Engineering Failure Analysis*, 26(0), 120-128. doi:<http://dx.doi.org/10.1016/j.engfailanal.2012.06.009>
- Sayer, R. J. (2013). *Operating Deflection Shapes, Part 2: Case History Applications*. Paper presented at the Proceedings of the Vibration Institute Training Conference and 37th Annual Meeting, Jacksonville, Florida.
- Schwarz, B. J., & Richardson, M. H. (1999). Introduction to operating deflection shapes. *CSI Reliability Week, Orlando, FL*.
- Semke, W. H., Bibel, G. D., Jerath, S., Gurav, S. B., & Webster, A. L. (2006). Efficient dynamic structural response modelling of bolted flange piping systems. *International Journal of Pressure Vessels and Piping*, 83(10), 767-776. doi:<http://dx.doi.org/10.1016/j.ijpvp.2006.06.003>
- Singh, P. K., Vaze, K. K., Bhasin, V., Kushwaha, H. S., Gandhi, P., & Ramachandra Murthy, D. S. (2003). Crack initiation and growth behaviour of circumferentially cracked pipes under cyclic and monotonic loading. *International Journal of Pressure Vessels and Piping*, 80(9), 629-640. doi:[http://dx.doi.org/10.1016/S0308-0161\(03\)00132-7](http://dx.doi.org/10.1016/S0308-0161(03)00132-7)
- Sukaih, N. (2002). A practical, systematic and structured approach to piping vibration assessment. *International Journal of Pressure Vessels and Piping*, 79(8-10), 597-609. Retrieved from <http://www.sciencedirect.com/science/article/B6V3N-4771TJ4-D/2/13ef01fc0999ddcbe507dcda37a4306d>
- Svein, S. (2011). Theoretical and experimental studies of stresses in flexible pipes. *Computers & Structures*, 89(23-24), 2273-2291. doi:10.1016/j.compstruc.2011.08.008
- Tang, Z., Lu, Z., Li, D., & Zhang, F. (2011). Optimal design of the positions of the hoops for a hydraulic pipelines system. *Nuclear Engineering and Design*, 241(12), 4840-4855. doi:10.1016/j.nucengdes.2011.08.058
- Thomas, P. J. (1999). *Simulation of industrial processes for control engineers*: Elsevier Science & Technology Books.
- Thomsen, J. J., & Dahl, J. (2010). Analytical predictions for vibration phase shifts along fluid-conveying pipes due to Coriolis forces and imperfections. *Journal of Sound and Vibration*, 329(15), 3065-3081. doi:<http://dx.doi.org/10.1016/j.jsv.2010.02.010>

- Tijsseling, A. S. (1996). FLUID-STRUCTURE INTERACTION IN LIQUID-FILLED PIPE SYSTEMS: A REVIEW. *Journal of Fluids and Structures*, 10(2), 109-146. Retrieved from <http://www.sciencedirect.com/science/article/B6WJG-45NJPGH-1/2/bc4edb6e5ee970fe658187584fcb59f6>
- Tijsseling, A. S. (2007). Water hammer with fluid-structure interaction in thick-walled pipes. *Computers & Structures*, 85(11-14), 844-851. Retrieved from <http://www.sciencedirect.com/science/article/B6V28-4N4S0F5-1/2/49bb6187b6a9e4cca54caee48dcb8400>
- Tongue, B. H. (2002). *Principles of vibration*.
- Trebuňa, F., Šimčák, F., Huňady, R., & Pástor, M. (2013). Identification of pipes damages on gas compressor stations by modal analysis methods. *Engineering Failure Analysis*, 27(0), 213-224. doi:<http://dx.doi.org/10.1016/j.engfailanal.2012.08.024>
- Vepsä, A. S. (2008). *Operational Displacement Shape Based Estimation Vibration Borne Stress*. Paper presented at the IMAC-XXVI Conf. & Expo. On Struct. Dynamics.
- Vold, H., Schwarz, B., & Richardson, M. (2000). *Measuring operating deflection shapes under non-stationary conditions*. Paper presented at the Proceedings of the 18th International Modal Analysis Conference, Kissimmee, Florida.
- Wachel, J. (1981a). *Piping Vibration and Stress*. Paper presented at the Machinery Vibration Monitoring and Analysis Seminar, New Orleans.
- Wachel, J. (1981b). *Piping Vibration and Stress*.
- Wachel, J., Morton, S. J., & Atkins, K. E. (1990). *Piping vibration analysis*. Paper presented at the Proceedings of the 19th turbomachinery symposium.
- Wachel, J., & Smith, D. (1991). *Vibration Troubleshooting of Existing Piping Systems*. Paper presented at the Engineering Dynamics Inc. Seminar Presentation (July 1991).
- Wachel, J. C. (1995). *Displacement Method for Determining Acceptable Piping Vibration Amplitudes*. Paper presented at the Joint ASME/JSME Pressure Vessels and Piping Conference, New York.
- Wang, J., & Hu, H. (2006). Vibration-based fault diagnosis of pump using fuzzy technique. *Measurement*, 39(2), 176-185. doi:<http://dx.doi.org/10.1016/j.measurement.2005.07.015>
- Wilcox, D. C. (2008). Formulation of the kw turbulence model revisited. *AIAA journal*, 46(11), 2823-2838.

- You, J. H., & Inaba, K. (2013). Fluid–structure interaction in water-filled thin pipes of anisotropic composite materials. *Journal of Fluids and Structures*, 36, 162-173.
- Zhai, H.-b., Wu, Z.-y., Liu, Y.-s., & Yue, Z.-f. (2011). Dynamic response of pipeline conveying fluid to random excitation. *Nuclear Engineering and Design*, 241(8), 2744-2749. doi:10.1016/j.nucengdes.2011.06.024
- Zhang, L., Tijsseling, S. A., & Vardy, E. A. (1999). Fsi Analysis of Liquid-Filled Pipes. *Journal of Sound and Vibration*, 224(1), 69-99. Retrieved from <http://www.sciencedirect.com/science/article/B6WM3-45FKX7V-BK/2/1e44dfd52ed6245400cdf963adb59ba3>
- Zhang, L., Wang, T., & Tamura, Y. (2010). *A frequency–spatial domain decomposition (FSDD) method for operational modal analysis*. *Mechanical Systems and Signal Processing*, (24, 5).
- Zou, G., Cheraghi, N., & Taheri, F. (2005). Fluid-induced vibration of composite natural gas pipelines. *International Journal of Solids and Structures*, 42(3), 1253-1268.